

Investigating the effects of ischemic stroke and diaschisis on connectomic presynaptic dendritic spine networks

by

Jenna Butterworth
B.Sc., University of Victoria, 2022

A Thesis Submitted in Partial Fulfillment
of the Requirements for the Degree

MASTER OF SCIENCE

in the Division of Medical Sciences (Neuroscience)

©Jenna Butterworth, 2024

University of Victoria

All rights reserved. This thesis may not be reproduced in whole or in part, by photocopy or other means, without the permission of the author.

We acknowledge and respect the Lək^wəŋən (Songhees and Esquimalt) Peoples on whose territory the university stands, and the Lək^wəŋən and W̱SÁNEĆ Peoples whose historical relationships with the land continue to this day.

Supervisory Committee

Investigating the effects of ischemic stroke and diaschisis on connectomic presynaptic dendritic spine networks

by

Jenna Butterworth
B.Sc., University of Victoria, 2022

Supervisory Committee

Dr. Craig E. Brown (Division of Medical Sciences)
Supervisor

Dr. Leigh Anne Swayne (Division of Medical Sciences)
Departmental Member

Dr. Brian Christie (Division of Medical Sciences)
Departmental Member

Abstract

Ischemic stroke is a life-threatening medical condition that can lead to dysfunction in brain regions both proximally and distally connected to the stroke site, a phenomenon known as “diaschisis”. Diaschisis can play an important role in recovery after stroke; however, the structural changes that occur at the level of neurons connected to the stroke site are not fully understood. Here, we performed confocal microscopy to visualize dendritic spines after a photothrombotic stroke in the primary somatosensory forelimb cortex (S1FL) of adult mice labeled with a retrograde adeno-associated virus (retro pAAV.CAG.GFP). This allowed for the visualization of presynaptic neurons directly connected to the infarct core in areas such as S1FL, motor cortex (MC), secondary somatosensory cortex (S2), and contralateral primary somatosensory forelimb cortex (Contra-S1FL). We observed a decrease in presynaptic spine density one week after stroke in superficial basilar dendrites within the peri-infarct region, which recovered by six weeks after stroke. An increase in dendritic spine density was also found six weeks after stroke within superficial primary apical dendrites in peri-infarct region, and within S2 in superficial primary and secondary apical dendrites as well as deep basilar dendrites. These results suggest that a retrograde degenerative signal may be localized to the peri-infarct region, whereas other factors may be playing a role in the widespread functional changes seen after stroke. The increase in dendritic spines seen in the peri-infarct and S2 regions six weeks after stroke may be playing an adaptive or compensatory role and aiding in recovery. Using a diaschisis model, these findings add novel information about neuronal structure proximal and distal to the infarct core, as well as elucidate potential degenerative and protective structural processes that may underly recovery after stroke.

Table of Contents

<i>Supervisory Committee</i>	<i>ii</i>
<i>Abstract</i>	<i>iii</i>
<i>Table of Contents</i>	<i>iv</i>
<i>List of Tables</i>	<i>vii</i>
<i>List of Abbreviations</i>	<i>viii</i>
<i>Acknowledgments</i>	<i>ix</i>
<i>1. Introduction</i>	<i>1</i>
<i>1.1 Stroke</i>	<i>1</i>
1.1.1 Clinical Population.....	1
1.1.2 Animal Models of Stroke.....	2
1.1.3 Mechanisms of Recovery Post Stroke.....	3
<i>1.2 Diaschisis and The Effects of Stroke on the Brain Connectome</i>	<i>4</i>
1.2.1 The Brain Connectome	4
1.2.2 Impacts of Stroke and Diaschisis on the Connectome.....	6
1.2.3 Impacts of Stroke and Diaschisis on Neurons	9
<i>1.3 Role of Dendritic Spines</i>	<i>10</i>
1.3.1 Dendritic Spine Plasticity and Stroke	12
<i>1.4 Retrograde Labeling of Dendritic Spines</i>	<i>15</i>
<i>1.5 Research Rationale</i>	<i>17</i>
<i>2. Methods</i>	<i>19</i>
<i>2.1 Animals</i>	<i>19</i>
<i>2.2 Viral Injections</i>	<i>19</i>
<i>2.3 Photothrombotic Stroke</i>	<i>20</i>
<i>2.4 Tissue Processing</i>	<i>20</i>
<i>2.5 Confocal Imaging</i>	<i>21</i>
<i>2.6 Epi-fluorescent Imaging</i>	<i>21</i>
<i>2.7 Data Analysis</i>	<i>22</i>
<i>2.8 Statistics</i>	<i>23</i>
<i>3. Results</i>	<i>25</i>
<i>3.1 No sex differences in dendritic spine density 1 or 6 weeks after sham or stroke</i>	<i>27</i>
<i>3.2 No difference in dendritic spine density between 1-week and 6-week sham groups</i> ...	<i>28</i>
<i>3.3 Higher dendritic spine density in superficial cortical neurons compared to deep cortical neurons across all groups</i>	<i>29</i>
<i>3.4 Higher spine density in secondary apical dendrites compared to primary apical dendrites across all groups</i>	<i>31</i>

3.5 Changes in dendritic spine density after stroke specific to peri-infarct region and S2	33
3.5.1 Within MC, no changes in spine density 1-week or 6-weeks after stroke	33
3.5.2 Stroke-related changes in spine density in Peri-infarct/S1FL	36
3.5.3 Spine density increases in S2 cortex 6-weeks after stroke	38
3.5.4 No changes in spine density in contralateral S1FL cortex after stroke.....	41
3.6 Decrease 1-week after stroke in peri-infarct spines cannot be explained by the branching direction of the dendrite, size of the infarct or distance to the infarct	44
4. Discussion	46
4.1 Overview	46
4.2 Limitations.....	51
4.3 Future Directions	52
5. Conclusion.....	54
References	55
Appendix.....	76

List of Figures

Figure 1: Schematic representation of 4 brain regions within the connectome	6
Figure 2: Schematic representation of retrograde viral labeling and example connectomic projections	17
Figure 3: Schematic summary of the experimental timeline and procedures	27
Figure 4: Dendritic spine density does not differ between sexes throughout the brain in both 1-week and 6-week groups.....	28
Figure 5: Dendritic spine density does not differ between 1-week shams and 6-week shams	29
Figure 6: Significantly higher spine density in superficial neurons compared to deep neurons in the sham, 1-week stroke and 6-week stroke groups	30
Figure 7: Significant difference in spine density between primary and secondary apical dendrites in sham, 1-week stroke and 6-week stroke groups	33
Figure 8: Within MC, no changes in dendritic spine density 1-week or 6-weeks after stroke	36
Figure 9: Within S1FL, spine density decreased 1-week after stroke in superficial basilar dendrites and increased 6-weeks after stroke in superficial basilar dendrites and deep primary apical dendrites	38
Figure 10: Within S2, spine density increased 6-weeks after stroke in superficial apical dendrites and deep basilar dendrites	41
Figure 11: Within Contra-S1FL, no changes in dendritic spine density 1-week or 6-weeks after stroke.....	43
Figure 12: Spine density reduction in peri-infarct basilar dendrites 1-week after stroke is not affected by branching direction of the dendrite, size of the infarct or distance to the infarct	45
Figure 13: No significant difference in dendritic spine density counts between researchers	76

List of Tables

Table 1: Two-way ANOVA of primary apical spine density with Depth (superficial vs deep) and Experimental Group (sham vs 1-week stroke vs 6-week stroke) as factors	43
Table 2: Two-way ANOVA of secondary apical spine density with Depth (superficial vs deep) and Experimental Group (sham vs 1-week stroke vs 6-week stroke) as factors. Significant main effects are highlighted in bold.....	43
Table 3: Two-way ANOVA of basilar spine density with Depth (superficial vs deep) and Experimental Group (sham vs 1-week stroke vs 6-week stroke) as factors. Significant main effects are highlighted in bold.....	43
Table 4: Summary of neurons counted in superficial and deep cortical layers per brain 1-week post-sham and stroke.....	77
Table 5: Summary of neurons counted in superficial and deep cortical neurons per brain 6-weeks post-sham and stroke.....	77

List of Abbreviations

AAV: Adeno-Associated Virus

ANOVA: Analysis of Variance

CAG: Chicken β -Actin

Contra-S1FL: Contralateral Primary Somatosensory Forelimb Cortex

GFP: Green Fluorescent Protein

IOS: Intrinsic Optical Signal

MCA: Middle Cerebral Artery

MC: Motor Cortex

mL: Milliliter

mm: Millimeter

nm: Nanometer

NVC: Neuro-Vascular Coupling

OIB: Olympus Image Binary

PBS: Phosphate Buffered Saline

PFA: Paraformaldehyde

S1FL: Primary Somatosensory Forelimb Cortex

S2: Secondary Somatosensory Cortex

SD: Standard Deviation

SEM: Standard Error of the Mean

S.Q: Subcutaneous

μ L: Microliter

μ m: Micrometer

VSD: Voltage-Sensitive Dye

Acknowledgments

I would like to first thank my supervisor Dr. Craig Brown for giving me the opportunity to conduct research in a field that I am passionate about, and for providing his mentorship and guidance along the way. Coming from a different undergraduate background, I appreciate all the time and patience that came along with training me and am deeply thankful for all that I have learned and taken away from working in his lab.

I would like to thank my committee members Dr. Leigh-Anne Swayne and Dr. Brian Christie for their invaluable feedback and support throughout the last few years. I greatly appreciated all their time and knowledge shared with me. I would also like to sincerely thank the animal care team, as well as the DMS and NGP staff who assisted me throughout this degree.

Thank you to all the current and past Brown Lab members during my time in the lab: Myrthe, Kamal, Dominique, Dhwani, Tanaka, Frances, Adam, Taylor, Vasil, Sam, Emilie, Ana Paula, Ale, Pat and Sorabh. My highlights during this degree were because of your sense of humor, help, insight, and friendship (especially the lab outings and coffee runs). I would like to specially thank Pat and the girliepops for being there through my entire experience and for providing countless help throughout my project. I am so grateful to have had such an amazing group of individuals to work and learn beside. I also thank all my other friends in the Neuroscience Graduate Program, from volleyball teams to neurocafe you are all exceptional and I was so lucky to have such supportive peers around me.

Most importantly, to my family and friends, thank you for teaching me the meaning of dedication. Your love and support mean the world and I could not have achieved this degree without you.

1. Introduction

1.1 Stroke

1.1.1 Clinical Population

Strokes are a life-threatening neurological disorder characterized by either a blockage or rupture in the cerebrovascular, resulting in impaired blood flow and cell death. Strokes are the second leading cause of death in the world (Campbell et al., 2019; Kuriakose & Xiao, 2020; Feigin et al., 2022), contributing to 6.5 million deaths annually (Feigin et al., 2022). Over the last 20 years, the lifetime risk of stroke has increased by 50% impacting 1 in 4 people over the age of 25 (Feigin et al., 2022). This is in part due to the increase in average lifespan, which is a result of developments in medical interventions and technology. The rise in the prevalence of stroke makes it an increasingly important disorder to study and understand.

The two types of strokes include hemorrhagic and ischemic, and of these different types of strokes, ischemic strokes are the most common (Campbell et al., 2019; Kuriakose & Xiao, 2020; Feigin et al., 2022). Ischemic strokes are caused by an occlusion in a cerebral artery (Campbell et al., 2019), and account for approximately 80% of all strokes (Boehme et al., 2017). The occlusion in the affected artery leads to a narrowing of the blood vessel and a lack of blood flow (Kuriakose & Xiao, 2020), which causes immediate cell death in the impacted region (Brown et al., 2008). The middle cerebral artery (MCA) is the most commonly affected artery by ischemic stroke (Gerrow & Brown, 2017; Hui et al., 2024). The MCA is the largest branch of the internal carotid artery and supplies blood to a large part of the cerebral hemisphere including the primary somatosensory and motor cortices. Ischemic strokes account for 7.6 million strokes and are a

leading cause of disability worldwide (Feigin et al., 2022) due to devastating brain damage and functional deficits (Brown et al., 2007; C.-L. Yu et al., 2015). These functional impairments often include forms of sensory, motor and cognitive impairment (Brown et al., 2007; Connell et al., 2008; Cramer et al., 2023).

The severity of the deficits caused by stroke can change rapidly within a short time frame. The typical stroke patient loses approximately 1.9 million neurons each minute a stroke is left untreated (Saver, 2006), making it imperative that individuals seek healthcare immediately. The goal of treatment is to restore blood flow to the affected regions, which can minimize the effects of ischemia if reperfusion is established quickly after onset (Chugh, 2019; Hui et al., 2024). Although the impacts of stroke occur rapidly, there is often restitution of some function in the weeks to months after the stroke indicating that the brain is capable of adapting after injury (Gerrow & Brown, 2017; Branco et al., 2019). Due to the heavy impact on neurons after stroke, it is vital to understand how these brain cells are impacted, and potentially adapting to assist with functional recovery after stroke. Over the past decade, stroke research has focused on investigating these potential cellular mechanisms that underlie this brain plasticity in order to generate therapies and mitigate functional deficits.

1.1.2 Animal Models of Stroke

In order to study the effects of stroke and subsequent plasticity, animal models are advantageous. This is due to the need for direct access to brain tissue, as well as the unpredictable nature of stroke in humans (Kuriakose & Xiao, 2020). A frequently used technique to model stroke in animals is the photothrombosis model (Watson et al., 1985). This involves an injection of a photosensitive dye (rose-bengal) that is activated by a laser leading to the production of reactive-oxygen species and platelet aggregation. The accumulation of these cells ultimately leads to an

occlusion in the targeted vessel. Although other models of stroke such as the occlusion of the MCA (MCAo) may be a more accurate representation of stroke in humans, there are limitations to the MCAo model due to the invasive procedure involved, the minimal control over the lesion volume and subsequent behavioural deficits (Carmichael, 2005; Gerrow & Brown, 2017). The photothrombotic model is advantageous due having more control over the location and size of the stroke, being less invasive and highly reproducible (Brown et al., 2007; C.-L. Yu et al., 2015; Kuriakose & Xiao, 2020). Inducing a stroke in animal models allows for the studying of functional and structural changes following stroke and enables researchers to investigate mechanisms of recovery.

1.1.3 Mechanisms of Recovery Post Stroke

Stroke leads to a cascade of structural and functional changes, which in turn alters behaviour, and although lost neurons cannot be replaced, the brain can exhibit certain forms of plasticity after a stroke allowing for the partial restoration of lost functions. The surviving tissue surrounding the stroke site termed the “peri-infarct” has been heavily researched due to its similar function and proximity to the infarct zone.

Previous research has established that after stroke, structural changes occur within the peri-infarct region such as dendritic spine turnover, axonal sprouting and synaptic plasticity, which play a crucial role in the formation of new neural connections (Stroemer et al., 1995; Carmichael et al., 2001; Dancause et al., 2005; Overman et al., 2012). The peri-infarct region may be primed to promote these changes due to growth proteins and factors, providing an enriched environment for structural plasticity and associated recovery (Murphy & Corbett, 2009; S. Li et al., 2010).

Imaging studies in humans and mice have revealed that functional changes also occur after stroke. A study utilizing *in vivo* intrinsic optical signal (IOS) and voltage-sensitive dye (VSD)

imaging revealed a decrease in response 1-week after stroke in the peri-infarct, which recovered after 8-weeks with the return of evoked depolarizations within the peri-infarct and neighboring regions (Brown et al., 2009). Another study used two-photon *in vivo* calcium imaging 1-2 months after a photothrombotic stroke targeted to forelimb primary somatosensory cortex (S1FL) and found that more neurons in the neighboring hindlimb primary somatosensory (S1HL) region were responding to forelimb stimulation (Winship & Murphy, 2008), providing direct evidence of functional remapping. Functional remapping in the peri-infarct cortex may occur due to structural changes that facilitate synapse formation and circuit reorganization (Gerrow & Brown, 2017; Campos et al., 2023). Functional reorganization and normalization of the activity of surviving neurons and pathways have been shown to aid in the recovery of function (Castro-Alamancos & Borrell, 1995; Dijkhuizen et al., 2001; Werhahn et al., 2003; Jaillard et al., 2005; Carmichael, 2006; Brown et al., 2007; Carmichael, 2012; Campos et al., 2023), and correlate with the behavioral recovery of sensory, motor and cognitive abilities (Castro-Alamancos & Borrell, 1995; Werhahn et al., 2003; Gerrow & Brown, 2017). Although the peri-infarct is an essential brain area to investigate after stroke, the brain is highly interconnected. The effects of stroke and recovery are not limited to the peri-infarct and have been shown to extend beyond the infarct core (Campos et al., 2023). As such, it is essential to study the brain as a “connectome” in order to fully unveil the underlying effects of stroke to understand and combat functional deficits.

1.2 Diaschisis and The Effects of Stroke on the Brain Connectome

1.2.1 The Brain Connectome

The term brain “connectome” was brought to light by Sporns to describe the neural connections/wiring diagram of the entire brain (Sporns et al., 2005). The connectome is currently

thought about in 3 scales: microscopic (at the level of synapses ex. dendritic spines), mesoscopic (at the level of regional connections ex. motor and primary somatosensory connections) and macroscopic (at the level of brain wide connections ex. thalamocortical connections) (Silasi & Murphy, 2014). Early studies in humans used imaging techniques such as resting state functional connectivity BOLD magnetic resonance imaging to understand brain connectivity in response to vascular and neuronal related disorders such as stroke (Carter et al., 2012); however, the details of neural projections cannot be studied at this macroscopic level. With recent advances in technology and analysis, researchers have been able to narrow in on the mesoscopic scale of the connectome and construct this wiring diagram in mice. An early method to visualize intracortical activity and neural connections involved *in vivo* channelrhodopsin-2 stimulation and regional VSD imaging, which showed the strong connections between many cortical areas, including the motor cortex (M1/M2), primary somatosensory forelimb cortex (S1FL), and secondary somatosensory cortex (S2) (Lim et al., 2012). Within the next few years, viral tracers were introduced to label neural connections and develop more extensive connectome maps. This included research that started the Mouse Connectome Project which used tracer injections to create a cortical connectivity atlas (Zingg et al., 2014). This atlas also highlighted the strong sensorimotor connections between motor cortex (M1/M2), primary somatosensory forelimb cortex (S1FL), secondary somatosensory cortex (S2) as well as their contralateral connections, and showed that each of these areas were extensively interconnected with each other (Zingg et al., 2014). Another group in the same year developed the Allen Mouse Brain Connectivity Atlas, which again focused on the mesoscopic connectome scale and used various viral tracers to enable whole brain mapping, and found this same connectivity between motor (M1/M2), primary/secondary somatosensory (S1/S2) and their contralateral counterparts (Oh et al., 2014) as displayed in Figure 1. These connectome maps are

extremely useful and important when it comes to fully comprehending the widespread deficits induced by stroke.

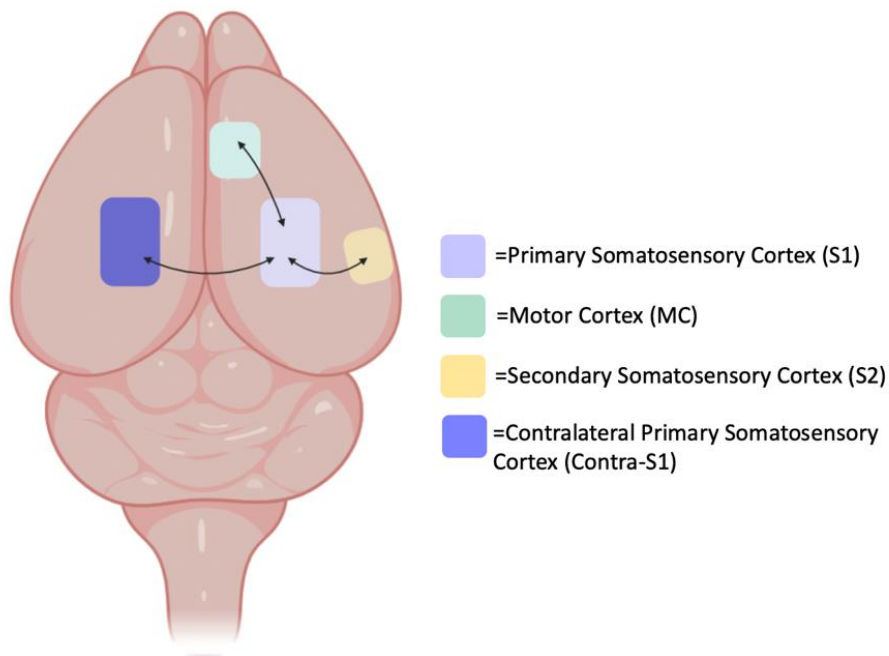


Figure 1: Schematic representation of 4 brain regions within the connectome

Schematic showing the bidirectional cortical connections of the primary somatosensory cortex (S1) with the motor cortex (MC), secondary somatosensory cortex (S2), and the contralateral primary somatosensory cortex (Contra-S1).

1.2.2 Impacts of Stroke and Diaschisis on the Connectome

Stroke mediated damage impacts the connections between neurons rapidly (Silasi & Murphy, 2014) and can lead to the disruption of function in areas distant from the site of damage, known as “diaschisis” (Silasi & Murphy, 2014; Carrera & Tononi, 2014). The term diaschisis was first coined by von Monakow (Finger et al., 2004; Carrera & Tononi, 2014) and can help to explain why we might see functional deficits in brain regions distant but connected to the infarct site. To highlight this concept, an example would be a patient experiencing motor deficits after having a stroke in the somatosensory cortex. Importantly, the brains surviving networks and circuitry can

compensate for the damaged area, which can improve functional recovery and serve as a promising therapeutic target (Silasi & Murphy, 2014). Collectively, this makes it vital to look at stroke and diaschisis through a connectomic approach as distant connected brain regions can undergo structural and functional changes after ischemia, providing important information about recovery.

The resulting diaschisis after stroke can impact many processes including neuronal connections, vasculature and metabolism, and neuro-vascular coupling. To add to this idea, human imaging data has shown strong linkages between neural connectivity and the outcome after stroke (Carter et al., 2012; Urbin et al., 2014), and recent electron microscopy studies have found dendritic degeneration and decrease in synaptic connections at sites connected to the infarct through diaschisis (Lee et al., 2020). Recent techniques have also utilized two-photon *in vivo* calcium imaging to demonstrate that stroke has impacts on both inhibitory and excitatory neurons connected to the infarct (Latifi et al., 2020). Therefore, it is no surprise that stroke and diaschisis can lead to structural and functional changes throughout the connectome. A way that the connectome may combat deficits after stroke is by using neural networks that are upstream and downstream (Murphy & Corbett, 2009) or contralateral from the infarct (Kokinovic & Medini, 2018) to assist in functional recovery.

Stroke also heavily impacts the vasculature of the brain and metabolism. When the occlusion of an artery causes the loss of connections to remote brain regions, the blood supply to these regions is impacted leading to subsequent loss of oxygen and nutrients supply downstream of the stroke site (Shih et al., 2013). Research in animals has used imaging techniques such as positron emission tomography to find a decrease in metabolic activity in regions adjacent to the infarct after stroke (Carmichael et al., 2004), demonstrating the metabolic consequences of diaschisis. One way to mitigate the vascular and metabolic disruption after stroke is to rapidly re-establish perfusion in

the impacted tissue (Schaffer et al., 2006; Juttler et al., 2006; Shih et al., 2009; Lay et al., 2010; Hermann & Chopp, 2012).

Due to the close-knit relationship of neurons and the cerebrovasculature, stroke has also been shown to impact neuro-vascular coupling (NVC). This is mediated by direct signaling from neurons to the vasculature, or by neural glutamate release to activate astrocytes that utilize Ca^{2+} signaling to influence nearby pericytes or vessels, leading to changes in microvascular hemodynamics after stroke (Mishra et al., 2016). NVC can be hindered acutely after stroke but serve as a protective factor during recovery. A pronounced neuro-vascular dissociation has been found after small-scale strokes, which is dependent on the extent of ischemia and results in prolonged neural deficits compared to a quicker restoration of cerebral blood flow (He et al., 2020). Although NVC can be disrupted immediately after stroke, it can also be utilized by the brain to facilitate functional restoration. Research investigating the impact of an ischemic stroke found that whisker stimulation within a critical time window protected mice from the MCAo (Lay et al., 2010). Another study found that after stroke, neurons expressed angiogenic factors to induce microvascular growth, and permit for regular blood flow to surviving and distant tissue post-stroke (Hermann & Chopp, 2012). Furthermore, a later study showed that sensory-related neural activity promoted the formation of vascular networks (Lacoste et al., 2014). Together these studies highlight the impact of NVC and the importance of connectomic neural networks. Overall, strokes are a disorder of the vasculature, but the vasculature and neural networks are highly interconnected, resulting in large scale changes in the peri-infarct and distant connected regions as well as pronounced impacts at the cellular level of the neuron.

1.2.3 Impacts of Stroke and Diaschisis on Neurons

Ischemic stroke leads to the deprivation of oxygen and energy that is needed by neurons, which in turn leads to the failure of the Na^+/K^+ pump and disruption of the resting membrane potential of neurons within the ischemic core. This results in a mass depolarization event that propagates through the brain, initiating from the ischemic core and propagating outward to the peri-infarct zone (Joshi & Andrew, 2001; Murphy & Corbett, 2009; Andrew et al., 2022; Campos et al., 2023). This depolarization event, termed spreading depolarization, occurs in regions where there is heavily metabolically compromised tissue and ultimately leads to neuronal damage and cell death (Joshi & Andrew, 2001; Andrew et al., 2022). The effect of spreading depolarization is reflected in research that has found that activity in peri-infarct pyramidal neurons is reduced for extended periods after stroke, known as neuronal “silencing” (Kokinovic & Medini, 2018; He et al., 2020). When spreading depolarization reaches tissue that was not originally damaged by the stroke, it is called spreading depression (Andrew et al., 2022). This neural depression in distant healthy tissue can potentially be linked to the diaschisis model of stroke (Finger et al., 2004; Campos et al., 2023). Combined, spreading depolarization and depression cause the destruction of neurons in the infarct core, damage to peri-infarct neurons, and longitudinal disruptions in connectivity and neural networks (Campos et al., 2023).

Recovery after stroke has been shown to be heavily reliant on plasticity-related changes occurring in the infarct periphery, as well as its connectomic inputs (Kokinovic & Medini, 2018). As such, the connectome plays a large role in stroke recovery, and it is therefore critical to understand the changes in connected neurons in both proximal and distal brain regions. A phenomenon that may contribute to neural plasticity after stroke is hyperexcitability, which is seen weeks to months after stroke. Hyperexcitability occurs due to the loss of inhibition as well as

electrophysiological changes in the affected neuronal populations after stroke, which facilitates a rich environment for axonal sprouting and the forming of new connections (Murphy & Corbett, 2009). Structural plasticity at the level of synapses in spared neurons may enable reconnections/remapping and potentiate functional recovery (Murphy & Corbett, 2009; Campos et al., 2023). Furthermore, the nervous system is a complex interconnected network that communicates through synaptic connections (Oh et al., 2014), and the location of these connections may elucidate important information about plasticity after stroke.

1.3 Role of Dendritic Spines

Dendritic spines are small protrusions located on neuronal dendrites and make up most of the excitatory synapses in the brain (Harris, 1999; Nimchinsky et al., 2002; Brown et al., 2007; Bhatt et al., 2009). These dendritic compartments contain neurotransmitter receptors, organelles and metabolic systems that are integral to chemical transmission (Nimchinsky et al., 2002; Lin et al., 2013). Dendritic spines are highly specialized for large Ca^{2+} signals (Nimchinsky et al., 2002), and the structure and functional regulation of the dendritic spine can therefore determine the strength of transmission that is sent to the connected receiving neuron (Lin et al., 2013). These dendritic spines have been proven to be very dynamic, and vary in sizes, shapes, and location within the brain (Karbowski & Urban, 2023).

Dendritic spines are found on distinct neurons in different regions throughout the brain. Spines are not limited to cortical regions but are also found in subcortical areas such as the striatum and cerebellum (Karbowski & Urban, 2023). Notably, dendritic spines are found on Purkinje cells within the cerebellum (Yuste & Bonhoeffer, 2004; Yuste, 2011; Karbowski & Urban, 2023), medium spiny neurons within the striatum (Deutch et al., 2007; Yuste, 2011), and pyramidal cells within the cortex (Yuste & Bonhoeffer, 2004; Yuste, 2011; Araya, 2014; Gemin et al., 2021).

Pyramidal cells are the most abundant type of neuron in the cerebral cortex, and almost 95% of excitatory synaptic inputs to these cells are received by dendritic spines (Araya, 2014). The cortex is the location of the sensory and motor cortices and subsequent connections, and as many forms of neurological disorders impact this sensorimotor functioning, the dendritic spines of cortical pyramidal cells are important to investigate.

The role of dendritic spines is highly diverse and morphological changes have been observed in both protective and pathological cases post-injury. Under normal conditions in healthy adults, dendritic spines have been shown to be relatively stable with little turnover (Grutzendler et al., 2002; Trachtenberg et al., 2002; Majewska & Sur, 2003; Zuo et al., 2005; Brown et al., 2007; Bhatt et al., 2009). Changes and plasticity in spines have been shown to depend on synaptic activity and can be modulated by experience (Kirov & Harris, 1999; Trachtenberg et al., 2002; Nimchinsky et al., 2002; Majewska & Sur, 2003; Kleim et al., 2004; Mizrahi et al., 2004; Holtmaat et al., 2006). Spines are also highly plastic during the development process (Zuo et al., 2005; Bhatt et al., 2009) as well as during learning and memory consolidation (Rakic et al., 1994; Lichtman & Colman, 2000; Gipson & Olive, 2017). For example, newly formed dendritic spines are formed within an hour of motor skill learning in living brain (X. Yu & Zuo, 2011). Due to the role dendritic spines play in learning and memory, it has been proposed that these compartments may be a structural location for long term information storage (Bhatt et al., 2009; Karbowski & Urban, 2023). Although dendritic spine dynamics have been shown to respond to experience, synaptic activity, learning, and memory, abnormal spines have also been implicated with injury and numerous brain disorders (Florence et al., 1998; Nimchinsky et al., 2002; Gao et al., 2011). The number and size of dendritic spines is regulated by gene products as well as the environment, making it very dynamic and malleable in nature and an important structural target for plasticity and recovery after

injury (Brown et al., 2007; Bhatt et al., 2009). It is therefore important to investigate dendritic spines in the context of stroke to further understand what is happening at the location of neural connections once they are disrupted.

1.3.1 Dendritic Spine Plasticity and Stroke

As dendritic spines are indicated as a potential marker of structural plasticity in the cortex, there is a surge in research investigating spine density in the context of stroke. Early research looking at the structural impacts of stroke established that there is a change in dendritic structure and spines after ischemia (Gonzalez & Kolb, 2003; S. Zhang et al., 2005; Corbett et al., 2006; S. Zhang & Murphy, 2007). Specifically, research focused on the peri-infarct region, as areas adjacent to the infarct are heavily impacted. It is well established that dendritic spines often experienced an acute decrease in density after stroke (Brown et al., 2007, 2008; Murphy & Corbett, 2009; Mostany et al., 2010; Joy et al., 2019), which is followed by a proliferation of spines weeks to months later during recovery (Brown et al., 2007; Murphy & Corbett, 2009; Mostany et al., 2010; Joy et al., 2019). Studies using *in vivo* two-photon imaging elucidate the plastic nature of dendritic spines by showing the remapped peri-infarct region had higher levels of dendritic spine turnover (Brown et al., 2009), and apical dendritic arbor remodeling increased within the first two weeks post-stroke (Brown et al., 2010). Similarly, research has found a decrease in spine density within the first 24 hours after stroke; however, the remaining spines were longer in length, which is theorized to be a potential process of plasticity to avoid excitotoxicity spreading to the soma and resulting in cell death (Brown et al., 2008). The effects of stroke on spines were found to be consistent in pyramidal neurons across cortical layers (Brown et al., 2008). Researchers also recognized the importance of looking at other brain regions, however there is a lot of contradicting results within the literature. Many studies found that there were either no changes in dendritic

structure or dendritic spines after stroke in regions distant to the infarct (Papadopoulos et al., 2006; Brown et al., 2007; Enright et al., 2007; Brown et al., 2008; Johnston et al., 2013; Tu et al., 2022; Merino-Serrais et al., 2023). On the other hand, there have been a few publications discussing the structural remodeling of dendrites in the contralateral hemisphere after stroke (Takatsuru et al., 2013; Huang et al., 2018). The differences in these connectomic results may be due to the methodology of neuronal tracing. The changes in dendritic spines seen after stroke is a multifaceted process and may be attributed to different factors.

As dendritic spine plasticity within the peri-infarct and at times in distant regions is apparent within the research, it is vital to investigate why these changes occur. The decrease in dendritic spine density after stroke can be attributed to multiple factors such as inflammation, deafferentation, and spreading depolarizations/hypo-excitability. After ischemic stroke, diverse members of the immune system are involved in an inflammatory response such as neutrophils, macrophages, and microglia (Gülke et al., 2018; Haupt et al., 2024). Microglia are among the first to respond to stroke, and thus, their role as resident immune cells of the central nervous system can impact the structural and functional integrity of surrounding neurons (Gülke et al., 2018; Y. Zhang et al., 2022; Haupt et al., 2024). Among these impacts are the modification to dendritic spines (Y. Zhang et al., 2022; Haupt et al., 2024), which has been shown *in vivo* and *in vitro* (Prada et al., 2018). Another theory for the loss of dendritic spines after stroke is deafferentation. This occurs when neurons lose sensory input and may result in neural adaptations such as dendritic and axonal changes (Butz et al., 2009). Research has shown that deafferentation can lead to alterations in dendritic organization, and the loss of spines (Jones & Thomas, 1962; Mostany et al., 2010; Dorostkar et al., 2015). Another cause of dendritic remodeling after stroke is spreading depolarizations, and the resulting hypo-excitability/silencing of neurons. The spreading

depolarization waves that occur as a consequence of ischemic stroke have been shown to also result in the loss of dendritic structure and spines (Takano et al., 2007; Murphy et al., 2008; Risher et al., 2010). These waves also activate inflammatory cascades (Chung et al., 2016), which may lead to the pruning of dendritic spines by microglia. The impact of spreading depolarizations on the structural integrity of neurons can vary greatly depending on the distance to the infarct core (Strong et al., 2006), which coincides with research showing loss of dendritic spines can be specific to the peri-infarct. After spreading depolarizations post-stroke, a period of hypo-excitability occurs (Carmichael, 2012) where neural activity is reduced. This may also contribute to the decrease in synapses after ischemia. Interestingly, dendritic spines were found to decrease in the acute phases post-stroke but were found to proliferate in the chronic phase.

An important factor that may aid in the increase in dendritic spines after stroke is rapid reperfusion. Studies have found that once the tissue regained proper perfusion, the dendrites were able to recover (S. Zhang & Murphy, 2007; P. Li & Murphy, 2008; Mostany et al., 2010). *In vivo* two-photon imaging found that dendritic spines proximal to infarct core gradually returned to baseline levels; however, in distant regions (to infarct core) with preserved blood flow, spines recovered much faster, and even surpassed baseline density (Mostany et al., 2010). Another major mechanism by which spine density may increase after stroke is neuroplasticity. Research has found that alterations in dendritic structure correlates with plasticity and recovery after stroke. Studies that elucidated this mechanism revealed a recovery of spines (Brown et al., 2007; Mostany et al., 2010), changes in dendritic arbor remodeling (Brown et al., 2010), dendritic spine turnover (Brown et al., 2009) and spine length (Brown et al., 2008) after stroke. These homeostatic processes after stroke may help to return synaptic activity to normal, and thus, can be markers of structural plasticity (Murphy & Corbett, 2009; Gerrow & Brown, 2017). The neuroplasticity in regions

connected to (but distantly located from) the stroke site could serve as a compensation mechanism, which may explain an increase in dendritic spines of neurons distant from the infarct site. In summary, it has been established that dendritic remodeling is observed after stroke and may act as a form of plasticity, contributing to functional recovery, and therefore may be a promising therapeutic target.

It is important to note that the current contradicting research of spine alterations outside of the peri-infarct can in-part be explained by the lack of tracing directly connected neurons to the infarct. The recent development of viral tracers that can trace neurons presynaptic or postsynaptic to the infarct site may shed light on the true impact of ischemia on connected neurons throughout the brain.

1.4 Retrograde Labeling of Dendritic Spines

To fully investigate the structural changes to dendritic spines in distant brain regions from infarct site, it is important to ensure that the neurons being studied are in fact connected to the site of injury. This can be achieved by using tracers that label neurons directly connected to site of injection. Viral tracers; which facilitate the expression of fluorescent protein in cells, were recently introduced as an alternative to chemical tracers due to directional specificity and high level of protein expression (Callaway, 2005; Luo et al., 2008; Betley & Sternson, 2011; Nassi et al., 2015). Retrograde viruses work by labelling upstream neurons that innervate the injection site (Zingg et al., 2014), where the virus is taken up by axon terminals and transported to the soma (Saleeba et al., 2019) as shown in Figure 2. There are numerous types of viral retrograde tracers including pseudorabies virus (PRV), rabies virus (RV), and adeno-associated virus (AAV), which present a useful tool for the analysis of structural markers of specific neural pathways (Saleeba et al., 2019; Z. Li et al., 2021). In recent years, the AAV viral model has become a preferred method of

retrograde tracing due to its high efficiency and selectivity, rapid gene expression and low toxicity (Tervo et al., 2016; Saleeba et al., 2019). The retrograde AAV allows for the robust labelling of projection neurons (Tervo et al., 2016), which makes it a good candidate for studying neurological diseases (Saleeba et al., 2019).

Retrograde labelling techniques have been used to study dendritic spines following different types of neurological disease and injury. In particular, dendritic structure has been studied in retrogradely labelled neurons in the context of spinal cord injury, amyotrophic lateral sclerosis (ALS), axon injury and traumatic brain injury (TBI) (Ghosh et al., 2012; Jara et al., 2012; Nagendran et al., 2017; Empl et al., 2022). However, fewer studies have investigated the dendritic spine density of retrogradely labeled neurons after stroke. Multiple studies have utilized retrograde labelling to study corticospinal connections following stroke (Liu et al., 2009; Starkey et al., 2012; Wahl et al., 2017), however these studies did not use a connectome approach nor study dendritic spines. A study that did investigate dendritic spines after stroke in retrogradely labelled neurons focused on thalamocortical neurons, rather than looking at multiple regions throughout the brain (Tu et al., 2022). Therefore, there is a gap in the literature when looking at the impact of stroke on presynaptic dendritic spines throughout the connectome.

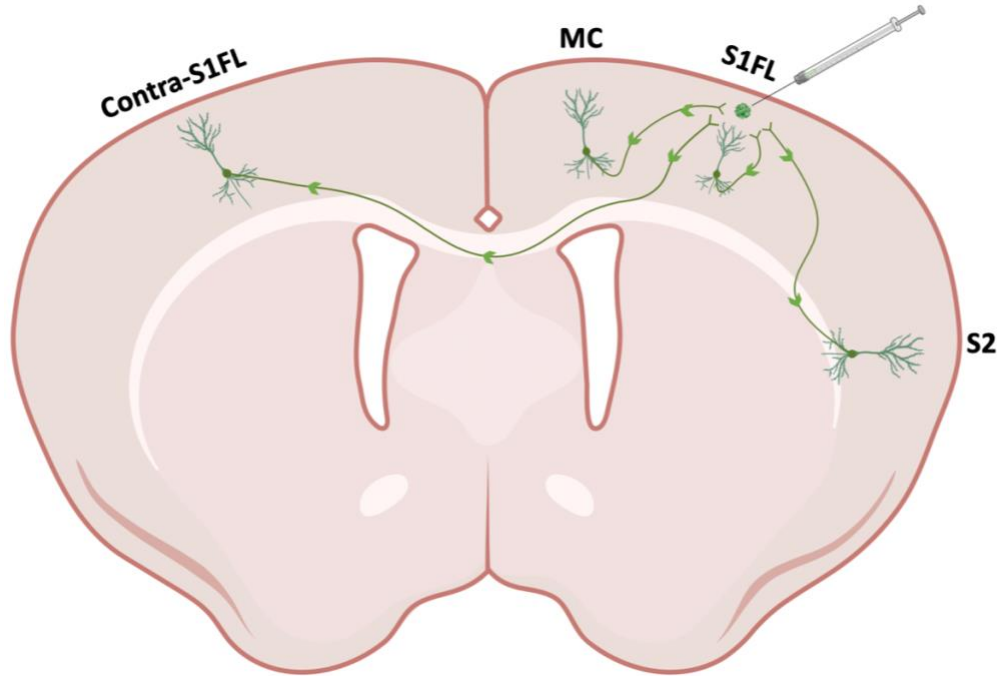


Figure 2: Schematic representation of retrograde viral labeling and example connectomic projections

Schematic showing an injection of a retrograde virus into the primary somatosensory forelimb (S1FL) region, which is taken up through the axons and transported to the soma and dendrites of neurons projecting to the injection site throughout the connectome. This results in neurons presynaptic to the injection site expressing a fluorescent protein in areas such as S1FL, the motor cortex (MC), secondary somatosensory cortex (S2) and contralateral primary somatosensory forelimb cortex (Contra-S1FL).

1.5 Research Rationale

Diaschisis following ischemic stroke can provide important information about recovery, as we often see dysfunction in brain regions distant from the infarct. However, the structural changes that occur in neurons directly connected to the stroke site are not fully understood. Previous research that has investigated dendritic spines after stroke have primarily focused on the peri-infarct region (Brown et al., 2007, 2008, 2009, 2010; Murphy & Corbett, 2009; Mostany et al., 2010; Joy et al., 2019), or regions that are functionally connected, but failed to trace directly connected neurons (Papadopoulos et al., 2006; Brown et al., 2007; Enright et al., 2007; Brown et

al., 2008; Johnston et al., 2013; Takatsuru et al., 2013; Huang et al., 2018; Tu et al., 2022; Merino-Serrais et al., 2023). This has led to contradictory results when studying the impacts of stroke on dendritic spine density in distant brain regions. It is therefore important to study directly connected neurons throughout the brain following stroke, which can be achieved using a retrograde AAV that labels presynaptic neurons. This neuronal tracer has been used to study dendritic spines following neurological issues such as TBI, axon injury, spinal cord injuries and ALS (Ghosh et al., 2012; Jara et al., 2012; Nagendran et al., 2017; Empl et al., 2022), but has been seldom used in the context of stroke and the brain connectome. Given this gap in the literature, this research aims to investigate the impacts of ischemic stroke on dendritic spine density in directly connected presynaptic neurons in multiple brain regions. This prompted our main research question:

Research Question: How is dendritic spine density affected in neurons projecting to the stroke site throughout the brain, 1-week and 6-weeks after ischemic stroke?

Hypothesis: Dendritic spine density in neurons that are upstream from the stroke site will be affected throughout the brain 1-week after stroke and will show recovery 6-weeks after stroke.

2. Methods

2.1 Animals

Six adult male and six adult female (2-3 months old) C57BL/6J mice were used for imaging neurons 1-week after stroke. For experiments investigating neurons 6-weeks after stroke, three adult male and five adult female (2-3 months old) C57BL/6J mice were used. The mice were housed in standard cages with unlimited access to water and a standard lab diet. The room was humidity controlled and maintained at $22.5^{\circ}\text{C} \pm 2.5^{\circ}\text{C}$, with a 12-hour light/dark cycle. All animals used for these experiments were cared for following university Animal Care Committee approved protocols and guidelines set by the Canadian Council on Animal Care (CCAC) standards.

2.2 Viral Injections

Mice were anesthetized with isoflurane (2% induction, 1.5% maintenance, 0.8 L/min flow) until sufficiently sedated and then fitted into a surgical stage. Liquid eye gel was then applied to prevent dryness. Animals were kept on a heating pad and body temperature was regulated at 37°C using a rectal thermoprobe and temperature feedback regulator. An injection of 0.05 mL of lidocaine using a 28-gauge insulin syringe was given subcutaneously (S.Q) above the skull to reduce any pain during/after the surgery. A midline incision was made along the scalp, and clamps were used to hold the skin back exposing the skull. A small hole was drilled using a high-speed dental drill above the primary somatosensory forelimb (S1FL) cortex (coordinates: 0mm anterior and 2.5 mm lateral of Bregma based on (Paxinos & Franklin, 2004) in the right hemisphere. Using a stereotaxic arm, a 32-gauge Hamilton syringe was then used to inject 0.2-0.4 μL of a retrograde AAV (retro pAAV.CAG.GFP, Addgene 37825-AAVrg.T, Titre: 2.2×10^{13} GC/mL) $\sim 800 \mu\text{m}$ deep into S1FL. The virus was diluted to 1:10 or 1:20 with filtered Phosphate Buffered Saline (PBS)

and 1 μ L of Alexa Fluor 568 in order to visualize the solution in the syringe. Following the injection, mice recovered from the anesthetic and were monitored under the heat lamp before being returned to their home cage.

2.3 Photothrombotic Stroke

After waiting a three-week period which allowed for the expression of the retrograde AAV, a photothrombotic stroke was targeted to the S1FL in the right hemisphere. Briefly, mice were anesthetized with isoflurane (2% induction, 1.5% maintenance, 0.8 flow) until sufficiently sedated and then fitted into a surgical stage. Liquid eye gel was used to prevent dryness, and animals were kept on the heating pad where body temperature was regulated at 37°C using a rectal thermoprobe and temperature feedback regulator. An injection of 0.05 mL of lidocaine was given S.Q above the skull to reduce pain. A midline incision was made along the scalp, and clamps were used to hold the skin back to expose the skull. A high-speed dental drill was used to thin an area of 1.5 mm x 1.5 mm of the skull above S1FL before giving an injection of rose bengal solution (100 mg/kg in cold Artificial Cerebrospinal Fluid (ACSF) buffer). The thinned S1FL area was then illuminated by a green laser (532 nm wavelength) for 10-15 minutes until the surface vessel stopped flowing. Sham control mice received either the injection of rose bengal without the illumination of green light, or the illumination of green light without the rose bengal. After the procedure, animals recovered under the heat lamp then were returned to their home cage.

2.4 Tissue Processing

At 1-week or 6-weeks post-sham or stroke, mice were anesthetized with an overdose of isoflurane (5%) and paw/tail reflexes were checked. Once sufficiently anesthetized, mice were transcardially perfused with 6 mL of 0.1M PBS and 6 mL of 4% paraformaldehyde (PFA). The

brains were extracted and preserved in 4% PFA overnight, before transferring to 0.1M PBS+0.02% azide the next day. The brains were then mounted and sliced on a vibratome (Leica VT1200S) into 100 μm thick coronal sections and stored in a 12-well plate with 0.1M PBS+0.02% azide. The sections were mounted on a gelatin-coated slide and coverslipped with Fluoromount-G (Southern Biotech).

2.5 Confocal Imaging

Pyramidal neurons at both superficial and deep cortical depths were imaged for this study. In each brain, five neurons from four brain regions were imaged. These regions consisted of the motor cortex (MC), primary somatosensory forelimb cortex (S1FL), secondary somatosensory cortex (S2), and contralateral to the primary somatosensory forelimb cortex (Contra S1FL). Perinfarct neurons were defined as $<1000\mu\text{m}$ from the infarct, due to minimal S1FL labelling in some stroke brains.

Images were obtained using a confocal microscope (Olympus Fluoview FV1000) with a 60x oil objective lens (NA= 1.35), and Olympus Fluoview software. Imaging specifications were as follows: zoom of 1.0, z-step of 0.6 μm , dwell time of 4.0 us/pixel, image size of 1600x1600 pixels, Kalman frame of 2. A laser centered at 488 nm wavelength with power ranging from 10-30% was used to illuminate the neurons.

2.6 Epi-fluorescent Imaging

An epifluorescence Olympus BX51 microscope with Olympus CellSens software was used with a 4x objective lens (NA= 0.13) to take low magnification images of the neurons imaged by the confocal, as well as image the stroke site. For acquiring infarct size images, a green fluorescent

protein (GFP) filter was used, and infarct sections were imaged from 2 brain wells that were sliced 300 μm apart (ex. Well 1 and Well 4).

2.7 Data Analysis

To assess dendritic spine density in stroke and sham animals, confocal image stacks were first blinded by another researcher and then opened in the program FIJI (ImageJ). Once the blinded Olympus image binary (OIB) files with an embedded scale (0.132 $\mu\text{m}/\text{pixel}$) were opened, four suitable dendrites were identified. When possible, a primary apical, secondary apical, primary basilar and secondary basilar dendrite were counted per neuron. The dendrites were selected by the following criteria: i) between 2-4 μm wide ii) had sufficient intensity to be countable iii) did not significantly overlap other dendrites to render more than 40% uncountable iv) had more than 30 μm of consecutive length for counting. The segmented line tool was used to trace along the dendrite for the entirety of the length that was to be counted and the length and max intensity value were recorded. To control for differences in labeling intensity, the maximum displayed value was set to 40% of the measured dendritic shaft intensity. The cell counter feature was then used to manually count spines along each dendrite using the following criteria: i) protruded from the shaft a minimum of 5 pixels/0.66 μm ii) was no more than 4 μm away from the dendritic shaft. The spine counting on the dendrite began at least 20 μm from the soma, as there were often very few spines found within the first 20 μm . In summary, the following values were recorded per dendrite: type (apical or basilar), branch order (primary or secondary), length of segment, number of spines, distance from soma, 40% of the max intensity value and z-plane. Additional variables such as the neuron's depth from the cortical surface or distance from the infarct were obtained using the 4x epi-fluorescent images. Neurons that were 450 μm or less from the cortical surface were considered superficial, whereas neurons more than 450 μm were considered deep.

In order to determine infarct volume, the 4x epi-fluorescent images were opened in FIJI and the scale was set to 456 pixels/mm. The infarct border was traced using the polygon tool, and the area (mm²) of the infarct was taken for each section in the two brain wells. The areas were then summed up and multiplied by 0.3 mm to account for the 300 μm distance between sections to estimate infarct volume (mm³).

Within the 1-week sample, 241 neurons were analyzed with approximately 50,000 spines counted (~1000 spines per area/~ 4000 spines per brain). Within the 6-weeks sample, 158 neurons were analyzed with approximately 37,000 spines counted (~1000 spines per area/~4000 spines per brain). **Table 4** and **Table 5** within the supplementary materials provide a summary of the superficial and deep cortical neurons counted within each brain, 1-week and 6-weeks after stroke.

2.8 Statistics

Statistical analysis for this study was performed using GraphPad Prism 10 software. Graphs are presented as mean ± standard deviation (SD). For analysis involving the comparison between groups (female vs male, sham 1-week vs 6-week, branch order analysis, superficial vs deep) across brain regions, a 2-way Analysis of Variance (ANOVA) was used. Similarly, a 2-way ANOVA was used for primary apical, secondary apical and basilar dendrites to compare groups (sham vs 1-week stroke vs 6-week stroke) across depth (superficial and deep) within each brain region. When significant, the 2-way ANOVA analyses were followed up with post-hoc t-tests (Šidák's multiple comparison test) to identify specific differences between groups. For the analysis of comparing basilar dendrites in the peri-infarct branching towards or away from the stroke site, an unpaired t-test was used. To identify the relationship between spine density in the peri-infarct and a) distance to the infarct and b) size of the infarct, a simple linear regression test was used. To ensure that the manual spine counting method was consistent across observers, a paired-t test was used to compare

spine density counts between two researchers (as shown by Figure 13 within supplementary material). The alpha value for all analyses were set at 0.05 (* $p < 0.05$, ** $p < 0.01$, *** $p < 0.001$, **** $p < 0.0001$).

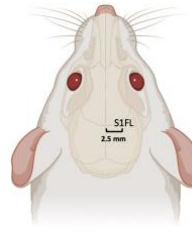
3. Results

In order to investigate spine density in retrogradely labelled neurons after stroke, 2–3-month-old C57BL6/J mice were injected with a retrograde AAV (retro pAAV.CAG.GFP). The timeline for these experiments is summarized below in Figure 3A. After viral injection into the S1FL region (as outlined in Figure 3B), the mice were allowed to recover for 3-weeks before inducing a photothrombotic stroke or sham stroke in this same area. The mice either then recovered for 1-week or 6-weeks before being perfused. Superficial and deep neurons were imaged within MC, S1FL, S2, and Contra-S1FL. Figure 3C provides a schematic representation of the brain regions, and Figure 3D provides a montage of retrograde labelling moving anterior to posterior through the brain in a sham and stroke mouse. The stroke was quantified using epi-fluorescent images as shown by Figure 3E. Dendritic spines were then manually counted using ImageJ.

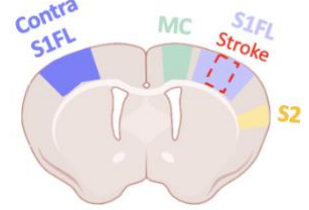
A.



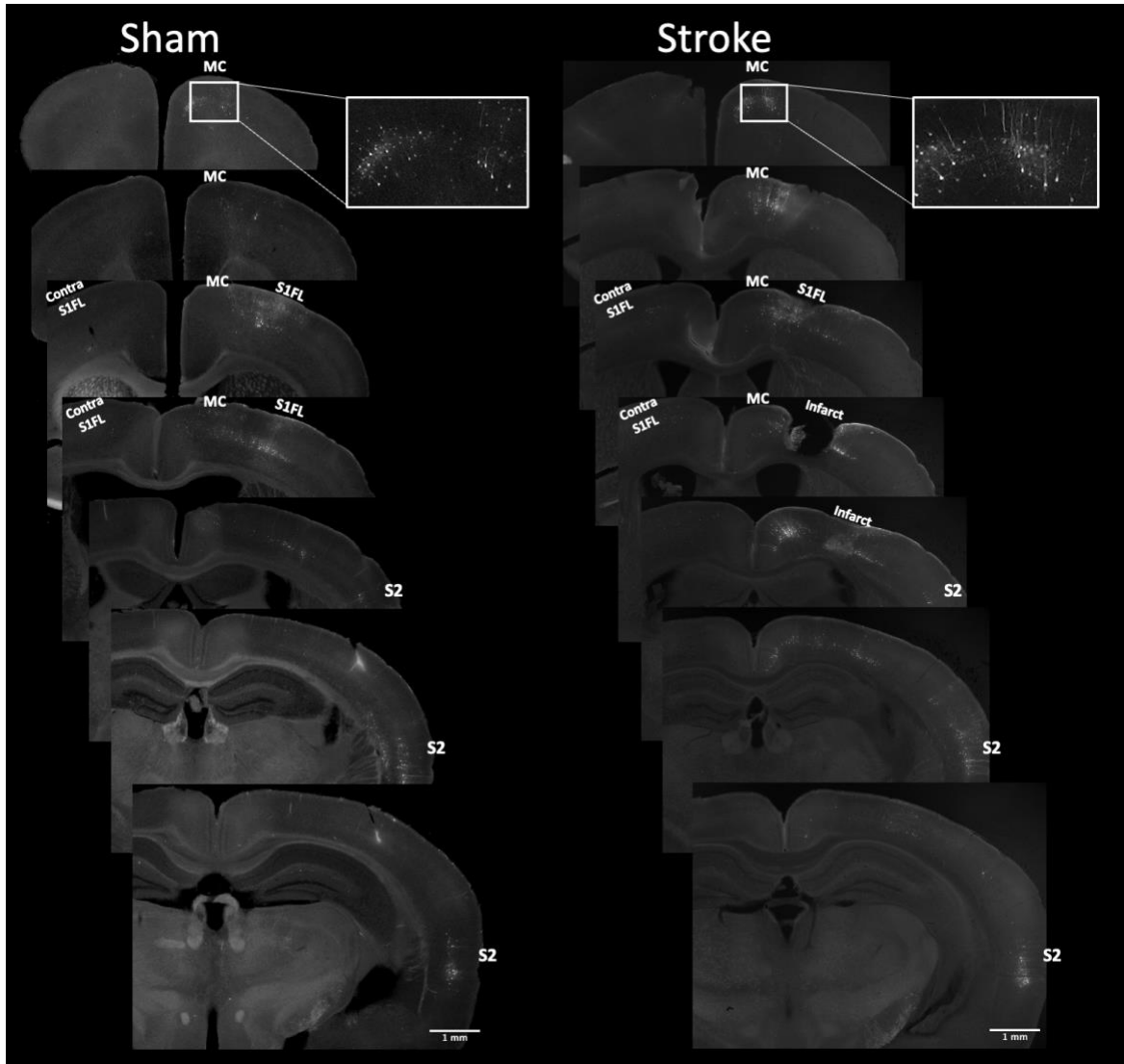
B.



C.



D.



E.

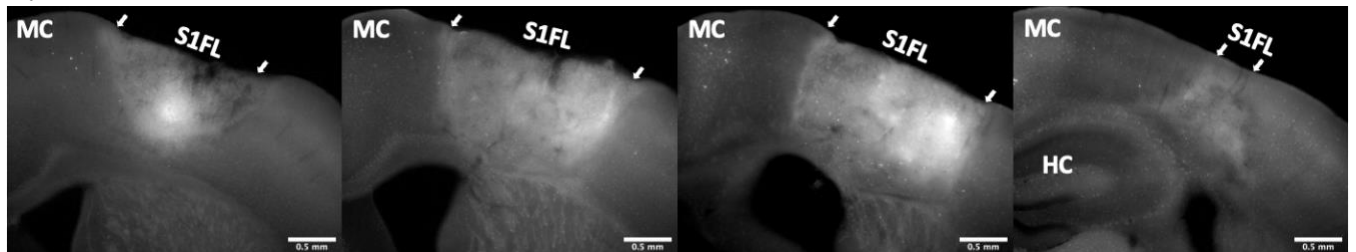


Figure 3: Schematic summary of the experimental timeline and procedures

A. Experimental timelines for imaging dendritic spine density 1-week post-stroke and 6-weeks post-stroke. **B.** Viral injections and photothrombotic stroke were targeted to S1FL in the right hemisphere (2.5 mm from bregma). **C.** Schematic of the brain regions that were imaged for this study; Motor Cortex (MC), Primary Somatosensory Forelimb (S1FL), Secondary Somatosensory (S2), Contralateral Primary Somatosensory Forelimb (Contra S1FL). **D.** Montage of the retrograde labelling throughout the brain moving anterior to posterior in both sham and stroke mice with an enlarged image of neurons in MC. The labelled brain regions correspond to the following: MC= Motor Cortex, S1FL= Primary Somatosensory Forelimb, S2= Secondary Somatosensory Cortex, Contra S1FL= Contralateral Primary Somatosensory Forelimb. **E.** Montage of the infarct moving anterior to posterior in the brain, with the borders of the infarct marked by the white arrows. The labelled brain regions correspond to the following: MC= Motor Cortex, S1FL= Primary Somatosensory Forelimb, HC= Hippocampus.

3.1 No sex differences in dendritic spine density 1 or 6 weeks after sham or stroke

First, we wanted to identify any potential sex differences in spine density within the experimental groups. To answer this question, we performed a 2-way ANOVA with sex and brain region as factors for both 1-week and 6-week sham and stroke groups. For the 1-week group, spine density was calculated per neuron in 3 females and 3 males per group. Within the sham group, analysis showed no significant effect of sex on spine density across brain regions (Figure 4A; main effect of sex: $F(1,113)=0.8564$, $p=0.3567$). The same analysis was conducted for the stroke group and also revealed no effect of sex on spine density (Figure 4B; main effect of sex: $F(1,112)=3.755$, $p=0.0552$). For the 6-week group, spine density was calculated per neuron in 2 females and 1 male in the sham group, and 3 females and 2 males in the stroke group. Both of these analysis also showed no significant effect of sex (Figure 4C; main effect of sex: $F(1,50)=2.202$, $p=0.1441$; Figure 4D; main effect of sex: $F(1,92)=3.683$, $p=0.0581$;). Due to there being no significant sex differences and to increase the power of the study, females and males were combined within 1-week and 6-week groups for further analysis.

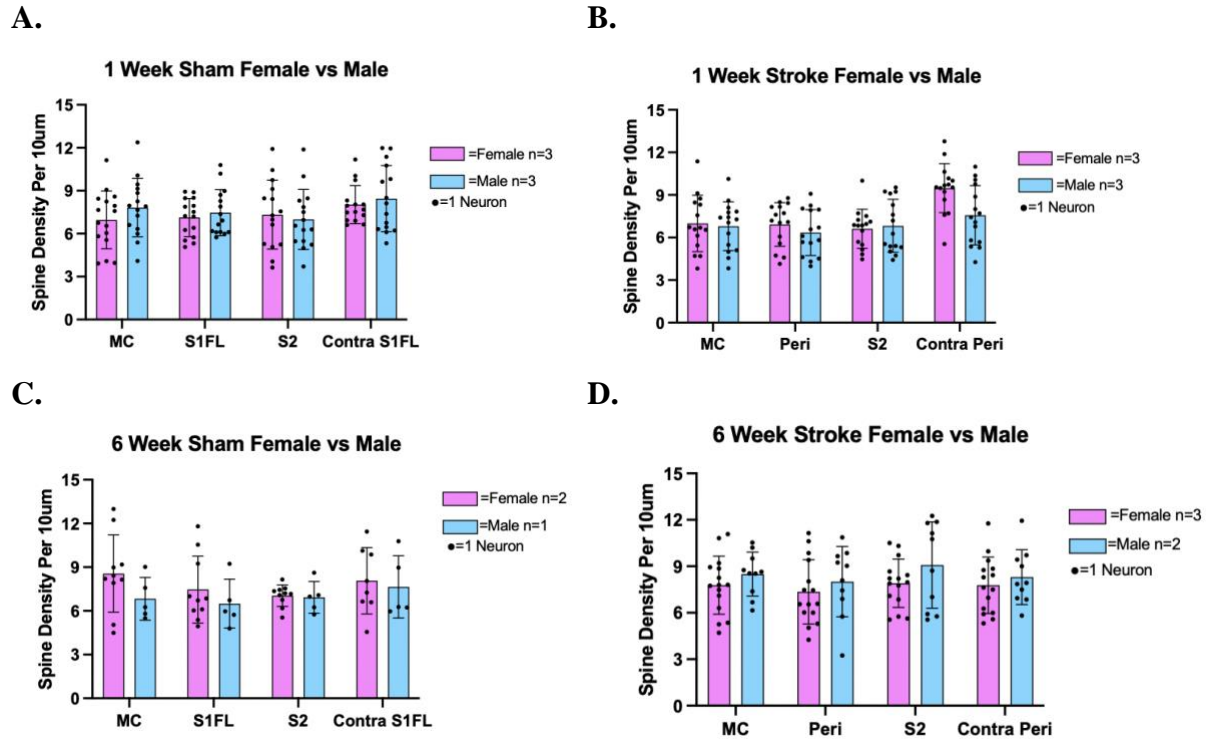


Figure 4: Dendritic spine density does not differ between sexes throughout the brain in both 1-week and 6-week groups

A. No significant differences between females (n=3) and males (n=3) across the four brain regions in the 1-week sham group. **B.** No significant differences between females (n=3) and males (n=3) across the four brain regions in the 1-week stroke group. **C.** No significant differences between females (n=2) and males (n=1) across the four brain regions in the 6-week sham group. **D.** No significant differences between females (n=3) and males (n=2) across the four brain regions in the 6-week stroke group. Error bars: mean±SD.

3.2 No difference in dendritic spine density between 1-week and 6-week sham groups

We then investigated any differences between the shams in the 1-week and 6-week groups. To do this, we conducted a 2-way ANOVA with group (sham 1-week vs sham 6-week) and brain region as factors. The analysis revealed no significant differences between the shams in any brain region (Figure 5; main effect of group: $F(1,171)=0.001673$ $p=0.9674$). Due to there being no significant differences and to increase power in the study, shams were pooled together for subsequent analysis.

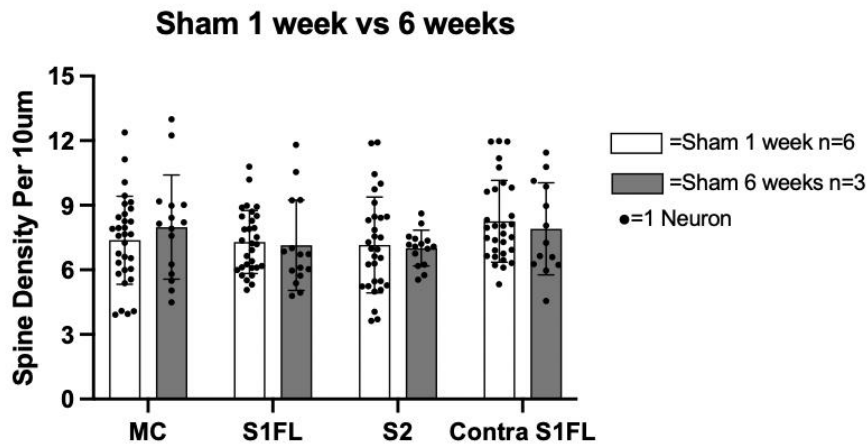


Figure 5: Dendritic spine density does not differ between 1-week shams and 6-week shams
 No significant differences between 1-week shams and 6-week shams across the four brain regions. Error bars: mean±SD.

3.3 Higher dendritic spine density in superficial cortical neurons compared to deep cortical neurons across all groups

Given that we sampled both superficial and deep cortical neurons in our study, we also wanted to test any differences between depths in each of our groups. A 2-way ANOVA was run for the sham (n=9), 1-week stroke (n=6) and 6-week stroke (n=5) groups with depth (superficial vs deep) and brain region as factors.

The sham group analysis revealed a significant main effect of depth (Figure 6A; main effect of depth: $F(1,171)=57.08, p<0.0001$ ***), with Šidák's multiple comparisons test revealing higher spine densities in superficial neurons compared to deep neurons in all the brain regions (MC $p=0.0032$ ** , S1FL $p=0.0001$ ***, S2 $p=0.0021$ ** , Contra-S1FL $p=0.0006$ ***).

The 1-week stroke group analysis also revealed a significant main effect of depth (Figure 6B; main effect of depth: $F(1,112)=37.69, p<0.0001$ ***), with Šidák's multiple comparisons test

revealing higher spine densities in superficial neurons compared to deep neurons in S1FL ($p=0.0051^{**}$), S2 ($p=0.0014^{**}$) and Contra-S1FL ($p=0.0001^{***}$).

Lastly, the 6-week stroke group continued this trend of a significant main effect of depth (Figure 6C; main effect of depth: $F(1,92)=25.21$, $p<0.0001^{****}$), with Šidák's multiple comparisons test revealing higher spine densities in superficial neurons compared to deep neurons in S2 ($p=0.0023^{**}$) and Contra-S1FL ($p=0.0446^{*}$). Given the significant difference in spine density between depth, further analysis was separated by superficial and deep neurons.

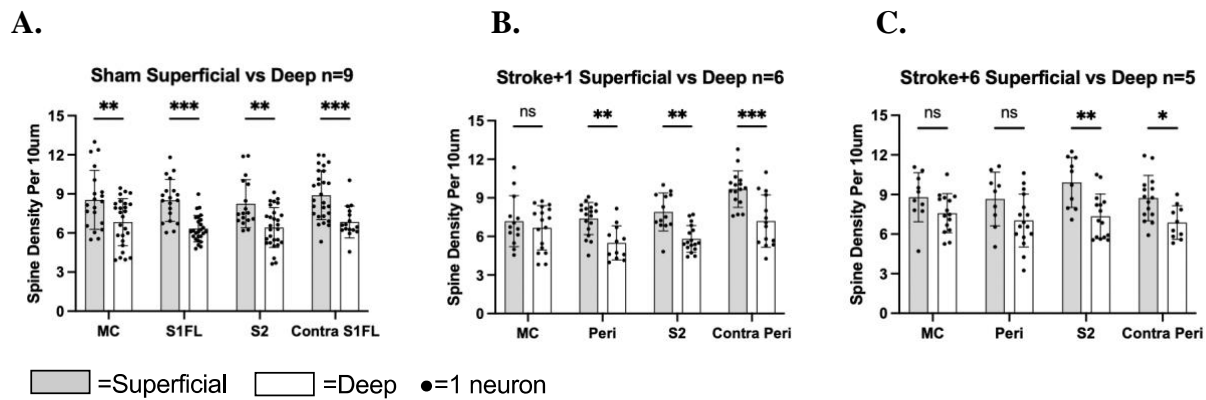


Figure 6: Significantly higher spine density in superficial neurons compared to deep neurons in the sham, 1-week stroke and 6-week stroke groups

A. In the sham group ($n=9$), higher spine density seen in superficial cortical neurons compared to deep cortical neurons in all brain regions. **B.** In the 1-week stroke group ($n=6$), higher spine density seen in superficial cortical neurons compared to deep cortical neurons in the Peri-infarct, S2 and Contra Peri-infarct. **C.** In the 6-week stroke group ($n=5$), higher spine density seen in superficial cortical neurons compared to deep cortical neurons in S2 and Contra-Peri. Error bars: mean \pm SD, * $p<0.05$, ** $p<0.01$, *** $p<0.001$.

3.4 Higher spine density in secondary apical dendrites compared to primary apical dendrites across all groups

To determine any differences in branch order within the sham, 1-week stroke and 6-week stroke groups, a 2-way ANOVA was conducted for apical and basilar dendrites with branch order (primary or secondary) and brain region as factors. Spine density was measured per dendrite in nine animals for the pooled sham group, six animals for the 1-week stroke group and 5 animals for the 6-week stroke group.

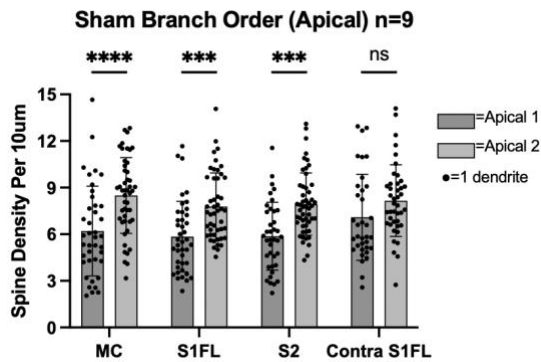
Within the sham group, my analysis revealed a significant effect of branch order in apical dendrites (Figure 7A; main effect of apical branch order: $F(1,335)=50.84$, $p<0.0001****$). Multiple comparisons indicated that secondary apical dendrites had significantly higher densities than primary apical dendrites in MC ($p<0.0001****$), S1FL ($p=0.0006***$) and S2 regions ($p=0.0002***$). On the other hand, the sham group showed no differences between branch order in basilar dendrites (Figure 7B; main effect of basilar branch order: $F(1,368)=0.2722$, $p=0.6021$).

Analysis within the 1-week stroke group also showed a significant effect of branch order in apical dendrites (Figure 7C; main effect of apical branch order: $F(1,223)=17.56$, $p<0.0001****$). Like the sham group, Šidák's test revealed higher spine densities in secondary apical dendrites compared to primary in MC ($p=0.0031**$). Similar to the sham group, the 1-week stroke group showed no differences between branch order in basilar dendrites (Figure 7D; main effect of basilar branch order: $F(1,241)=1.289$, $p=0.2574$).

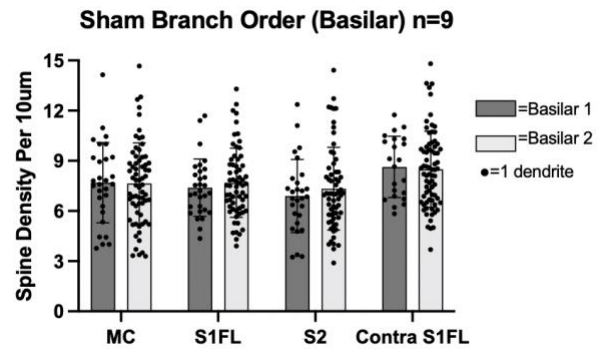
Analysis within the 6-week stroke group also revealed a significant effect of branch order in apical dendrites (Figure 7E; main effect of apical branch order: $F(1,184)=5.897$, $p=0.0161*$). Similar to the sham and 1-week stroke group, Šidák's multiple comparison test revealed higher spine densities in secondary apical compared to primary apical dendrites within S2 ($p=0.0384*$).

Like the other groups, the 6-week stroke group did not display any differences in basilar dendrites. (Figure 7F; main effect of basilar branch order: $F(1,198)=0.09956$, $p=0.7527$). Based on these results, subsequent data for spine density will present primary and secondary apical dendrites separately, whereas primary and secondary basilar dendrites will be pooled together.

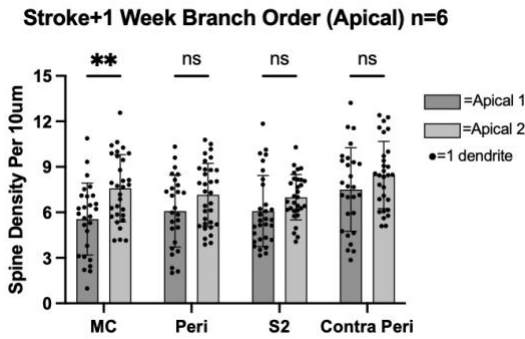
A.



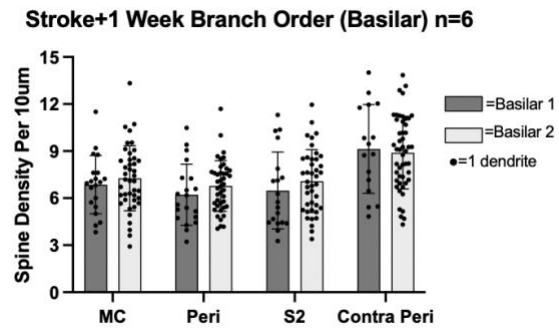
B.



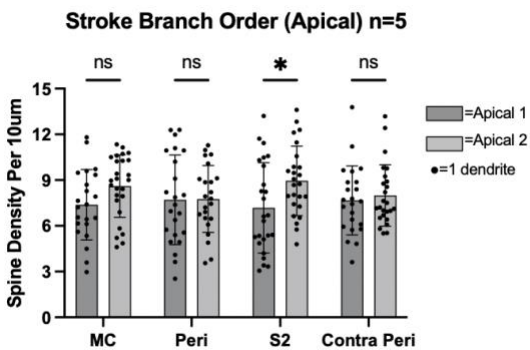
C.



D.



E.



F.

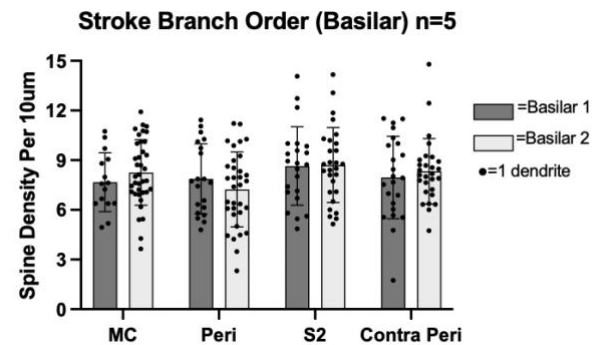


Figure 7: Significant difference in spine density between primary and secondary apical dendrites in sham, 1-week stroke and 6-week stroke groups

A. In the sham group (n=9), primary apical dendrites show significantly less spine density compared to secondary apical dendrites in MC, S1FL and S2. **B.** In the sham group (n=9), no significant differences were found between primary and secondary basilar dendrites. **C.** In the 1-week stroke group (n=6), primary apical dendrites show significantly less spine density compared to secondary apical dendrites in MC. **D.** In the 1-week stroke group (n=6), no significant differences were found between primary and secondary basilar dendrites. **E.** In the 6-week stroke group (n=6), primary apical dendrites show significantly less spine density compared to secondary apical dendrites in S2. **F.** In the 6-week stroke group (n=6), no significant differences were found between primary and secondary basilar dendrites. Error bars: mean±SD, * p<0.05, ** p<0.01, *** p<0.001, **** p<0.00001.

3.5 Changes in dendritic spine density after stroke specific to peri-infarct region and S2

The main question for this research project was to determine how spine density was affected after stroke in neurons that projected to the stroke site throughout the brain. A 2-way ANOVA was used to investigate this within each brain region, with experimental group (sham vs 1-week stroke vs 6-week stroke) and cortical depth (superficial vs deep) as factors and spine density displayed as an average per neuron for primary apical, secondary apical and basilar dendrites. All ANOVA results are reported for primary apical dendrites in **Table 1**, secondary apical dendrites in **Table 2**, and basilar dendrites in **Table 3**.

3.5.1 Within MC, no changes in spine density 1-week or 6-weeks after stroke

First, we investigated spine density in MC. Neurons were sampled from superficial and deep cortical layers in shams (as shown in Figures 8A-C). Dendritic spine density was counted in primary apical, secondary apical and basilar dendrites as displayed in Figures 8D-F. This was also conducted in the stroke groups, as visualized in Figures 8G-L. The analysis revealed a significant main effect of experimental group (sham vs 1-week stroke vs 6-week stroke) in primary apical

dendrites (Figure 8M; main effect of experimental group: $F(2,83)=4.387$, $p=0.0154^*$), however upon further investigation using Šidák's multiple comparisons test, no significant effects were found between groups in neither superficial nor deep neurons. The analysis revealed no significant main effect in secondary apical (Figure 8N; main effect of experimental group: $F(2,90)=2.534$, $p=0.0850$) or basilar dendrites (Figure 8O; main effect of experimental group: $F(2,95)=2.061$, $p=0.1330$).

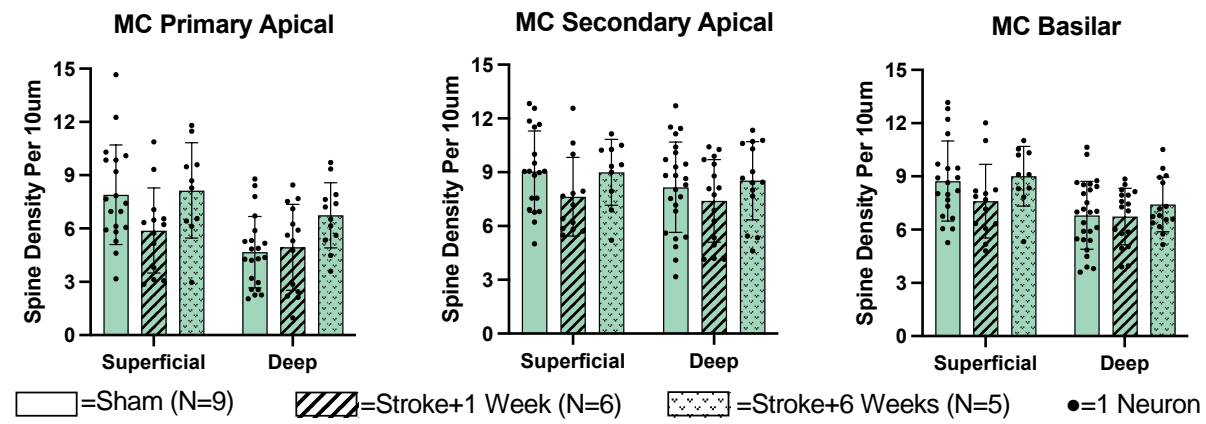
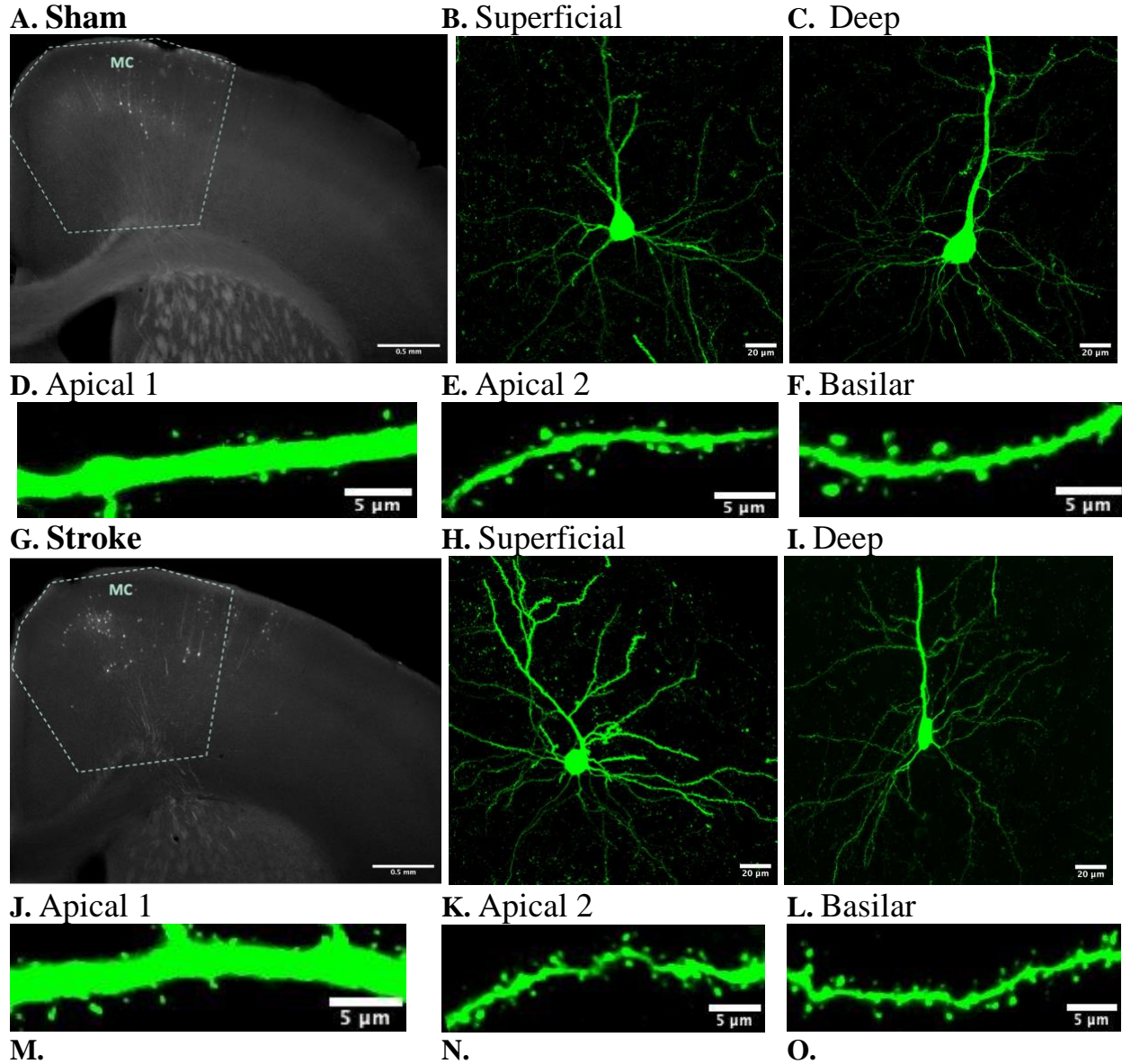
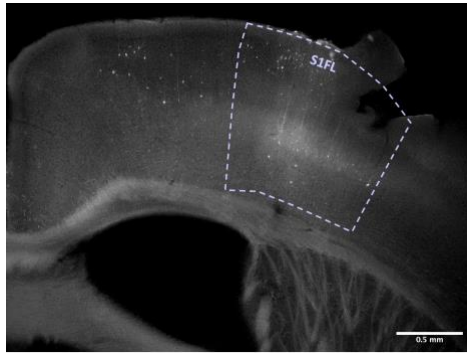


Figure 8: Within MC, no changes in dendritic spine density 1-week or 6-weeks after stroke
A-C. Retrogradely labelled neurons in MC region in both superficial and deep cortical depths within the sham group. **D-F.** Enlarged image of MC primary apical, secondary apical and basilar dendrite within the sham group. **G-I.** Retrogradely labelled neurons in MC region in both superficial and deep cortical depths after stroke. **J-L.** Enlarged image of MC primary apical, secondary apical and basilar dendrites 1-week after stroke. **M-O.** In primary apical, secondary apical, and basilar dendrites within MC, no changes in spine density were observed in superficial or deep layers 1-week or 6-weeks after stroke. Error bars: mean \pm SD.

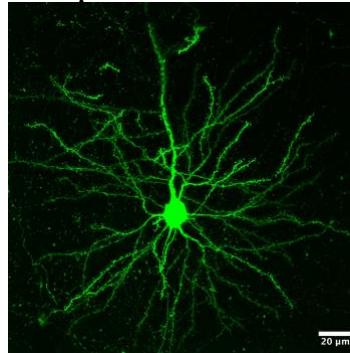
3.5.2 Stroke-related changes in spine density in Peri-infarct/S1FL

Next, we investigated spine density in S1FL/Peri-infarct neurons. As described with the MC analysis, neurons were sampled from superficial and deep cortical layers in shams (as shown in Figures 9A-C). Representative neurons and dendrites are shown for sham mice (Figures 9D-F) and 1 week stroke mice (Figures 9G-L). The analysis revealed a significant main effect of experimental group (sham vs 1-week stroke vs 6-week stroke) in primary apical dendrites (Figure 9M; main effect of experimental group: $F(2,83)=5.641, p=0.005^{**}$), multiple comparisons were conducted using Šidák's test to reveal a significant increase in spine density 6-weeks after stroke compared to the sham group ($p=0.02^*$) and 1-week stroke group ($p=0.01^*$) within deep neurons. The analysis revealed no significant main effect in secondary apical dendrites (Figure 9N; main effect of experimental group: $F(2,89)=1.919, p=0.15$), however revealed a significant main effect in basilar dendrites (Figure 9O; main effect of experimental group: $F(2,94)=8.581, p=0.0004^{***}$). Šidák's multiple comparisons test was conducted which showed a decrease in spine density 1-week after stroke compared to shams ($p=0.002^{**}$) and an increase in spine density 6-weeks after stroke compared to 1-week after stroke ($p=0.04^*$) in superficial neurons.

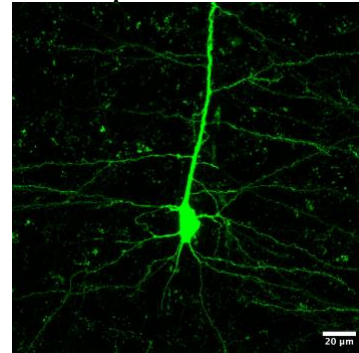
A. Sham



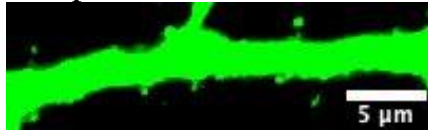
B. Superficial



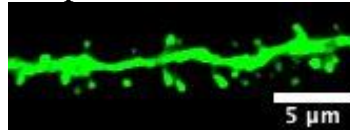
C. Deep



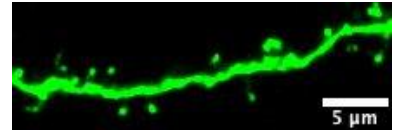
D. Apical 1



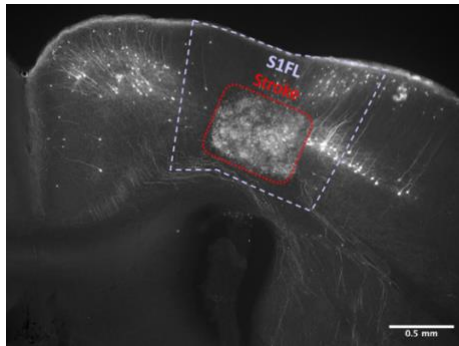
E. Apical 2



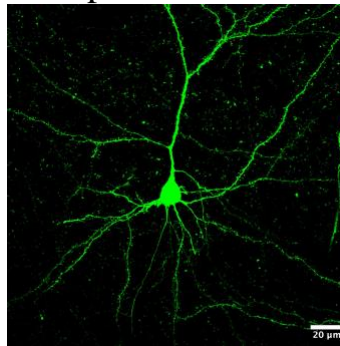
F. Basilar



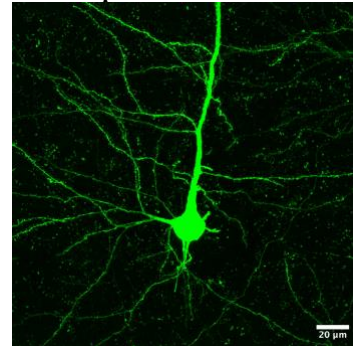
G. Stroke



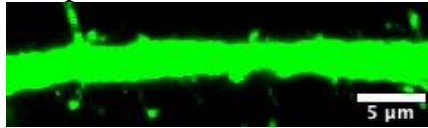
H. Superficial



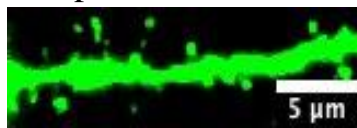
I. Deep



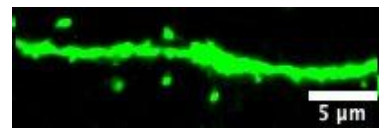
J. Apical 1



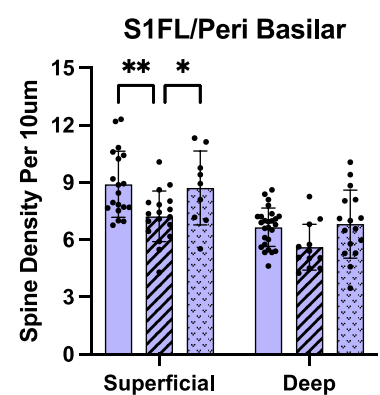
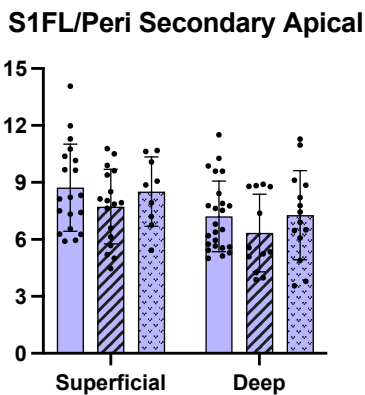
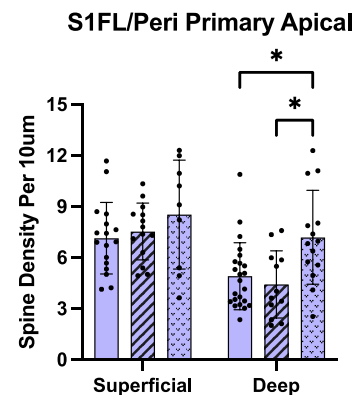
K. Apical 2



L. Basilar



M.



□ = Sham (N=9)

▨ = Stroke+1 Week (N=6)

▤ = Stroke+6 Weeks (N=5)

● = 1 Neuron

Figure 9: Within S1FL, spine density decreased 1-week after stroke in superficial basilar dendrites and increased 6-weeks after stroke in superficial basilar dendrites and deep primary apical dendrites

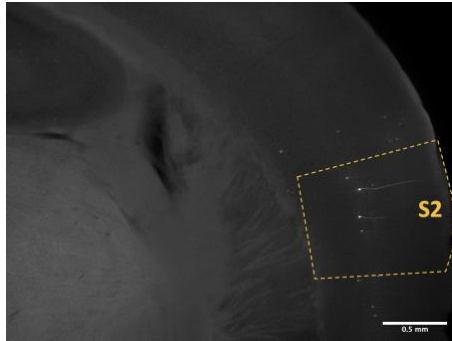
A-C. Retrogradely labelled neurons in S1FL region in both superficial and deep cortical depths within the sham group. **D-F.** Enlarged image of S1FL primary apical, secondary apical and basilar dendrite within the sham group. **G-I.** Retrogradely labelled neurons in Peri-infarct region in both superficial and deep cortical depths after stroke. **J-L.** Enlarged image of peri-infarct primary apical, secondary apical and basilar dendrites 1-week after stroke. **M.** In primary apical dendrites within S1FL/peri-infarct, spine density increased in deep neurons 6-weeks after stroke compared to 1-week after stroke and the sham group. **N.** No changes in spine density were observed in secondary apical dendrites within S1FL/peri-infarct. **O.** In basilar dendrites within S1FL/peri-infarct, spine density decreased in superficial neurons 1-week after stroke compared to shams, which recovered by 6-weeks after stroke. Error bars: mean±SD, * $p < 0.05$, ** $p < 0.01$.

3.5.3 Spine density increases in S2 cortex 6-weeks after stroke

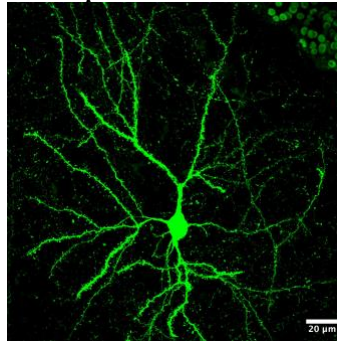
Neurons within the S2 region were sampled from superficial and deep cortical layers in shams (as shown in Figures 10A-C). Dendritic spine density was counted in primary apical, secondary apical and basilar dendrites as displayed in Figures 10D-F. This was also conducted in the stroke groups, as visualized in Figures 10G-L. The analysis revealed a significant main effect of experimental group (sham vs 1-week stroke vs 6-week stroke) in primary apical dendrites (Figure 10M; main effect of experimental group: $F(2,87)=4.540$, $p=0.0133^*$), and upon further investigation, it was revealed that spine density increased 6-weeks after stroke compared to the sham group in superficial neurons ($p=0.0301^*$). The analysis also revealed a significant main effect of experimental group (sham vs 1-week stroke vs 6-week stroke) in secondary apical dendrites (Figure 10N; main effect of experimental group: $F(2,92)=8.019$, $p=0.0006^{***}$), with an increase in spine density 6-weeks after stroke compared to 1-week after stroke in superficial neurons ($p=0.0043^{**}$). Similar to the other types of dendrite, the analysis revealed a significant main effect of experimental group (sham vs 1-week stroke vs 6-week stroke) in basilar dendrites (Figure 10O; main effect of experimental group: $F(2,94)=7.232$, $p=0.0012^{**}$). Šidák's multiple comparisons

showed an increase in spine density 6-weeks after stroke compared to 1-week after stroke in deep neurons ($p=0.0448^*$).

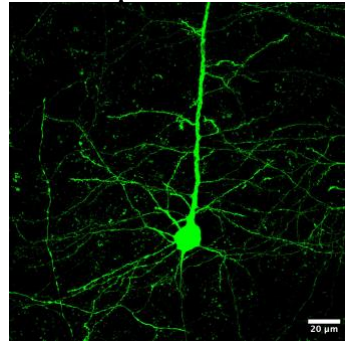
A. Sham



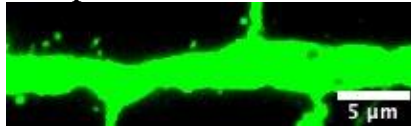
B. Superficial



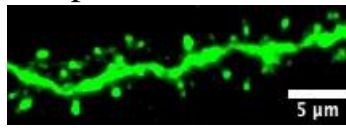
C. Deep



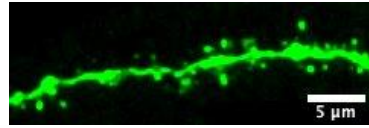
D. Apical 1



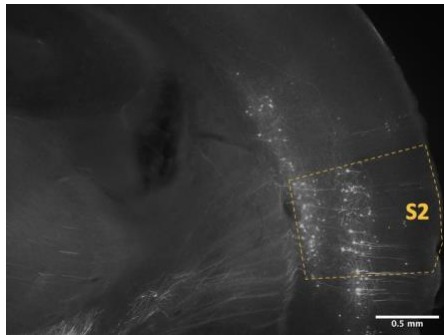
E. Apical 2



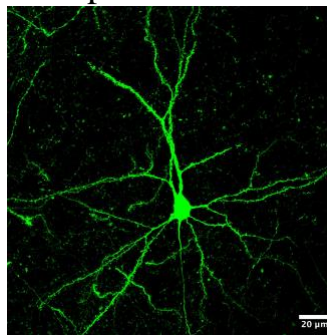
F. Basilar



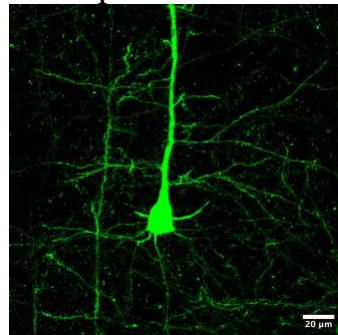
G. Stroke



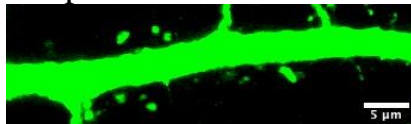
H. Superficial



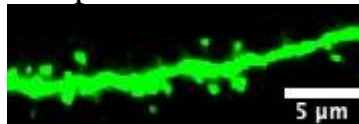
I. Deep



J. Apical 1



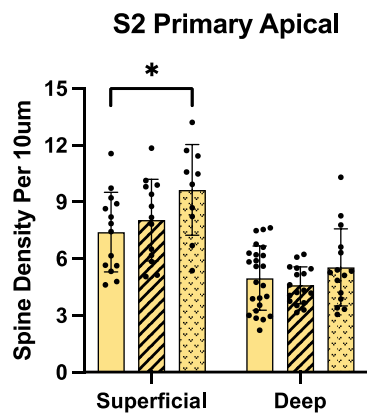
K. Apical 2



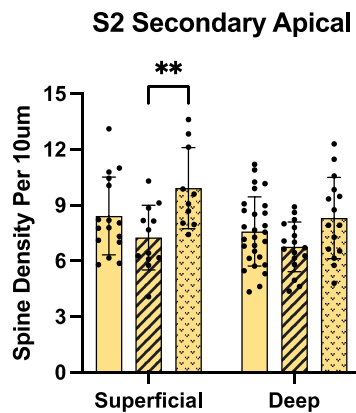
L. Basilar



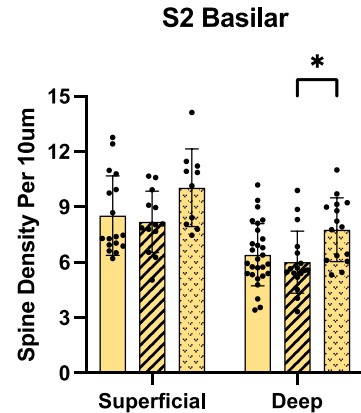
M.



N.



O.



□ = Sham (N=9)

▨ = Stroke+1 Week (N=6)

▤ = Stroke+6 Weeks (N=5)

● = 1 Neuron

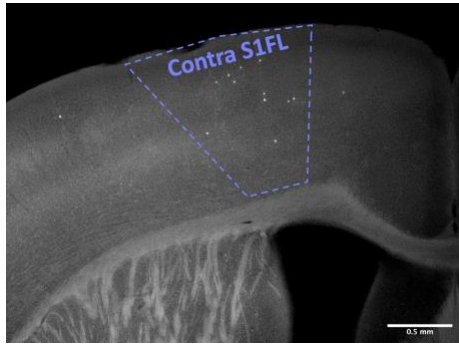
Figure 10: Within S2, spine density increased 6-weeks after stroke in superficial apical dendrites and deep basilar dendrites

A-C. Retrogradely labelled neurons in S2 region in both superficial and deep cortical depths within the sham group. **D-F.** Enlarged image of S2 primary apical, secondary apical and basilar dendrite within the sham group. **G-I.** Retrogradely labelled neurons in S2 region in both superficial and deep cortical depths after stroke. **J-L.** Enlarged image of S2 primary apical, secondary apical and basilar dendrites 1-week after stroke. **M.** In primary apical dendrites within S2, spine density increased in superficial neurons 6-weeks after stroke compared to shams. **N.** In secondary apical dendrites within S2, spine density increased in superficial neurons 6-weeks after stroke compared to 1-week after stroke. **O.** In basilar dendrites within S2, spine density increased in deep neurons 6-weeks after stroke compared to 1-week after stroke. Error bars: mean±SD, * $p<0.05$, ** $p<0.01$, *** $p<0.001$.

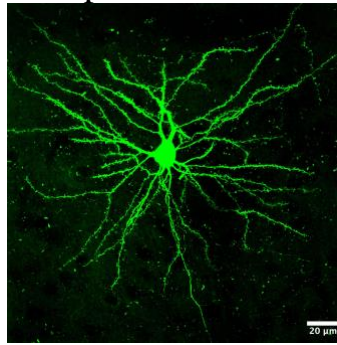
3.5.4 No changes in spine density in contralateral S1FL cortex after stroke

Lastly, we investigated spine density contralateral to the stroke (Contra-S1FL). As with the other areas, neurons were sampled from superficial and deep cortical layers in shams (as shown in Figures 11A-C). Dendritic spine density was counted in primary apical, secondary apical and basilar dendrites as displayed in Figures 11D-F. This was also conducted in the stroke groups, as visualized in Figures 11G-L. The analysis revealed no significant main effect of experimental group (sham vs 1-week stroke vs 6-week stroke) in primary apical (Figure 11M; main effect of experimental group: $F(2,79)=0.5159$, $p=0.5990$), secondary apical (Figure 11N; main effect of experimental group: $F(2,84)=0.2260$, $p=0.7982$), or basilar dendrites (Figure 11O; main effect of experimental group: $F(2,92)=1.974$, $p=0.1448$).

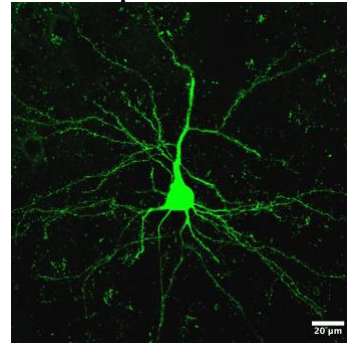
A. Sham



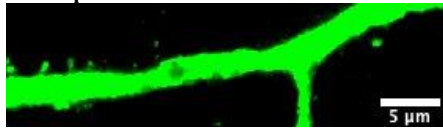
B. Superficial



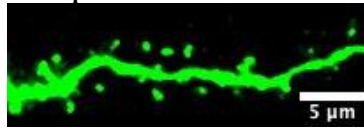
C. Deep



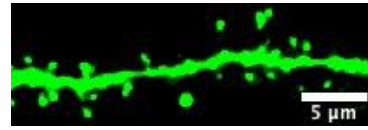
D. Apical 1



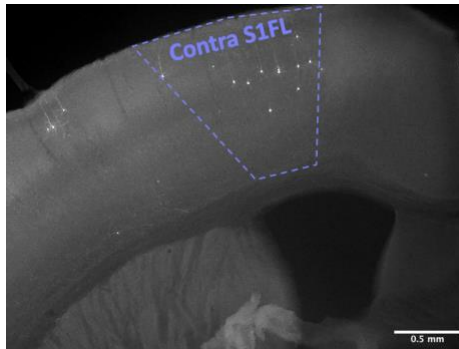
E. Apical 2



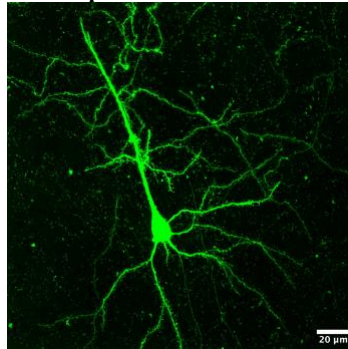
F. Basilar



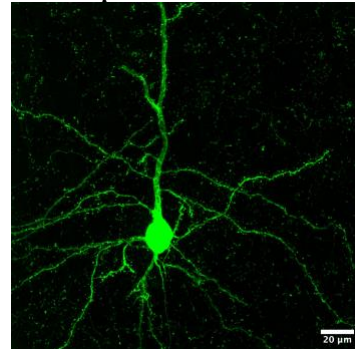
G. Stroke



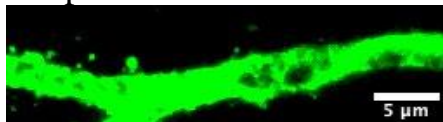
H. Superficial



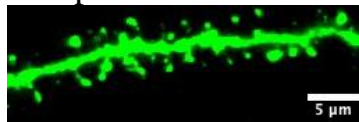
I. Deep



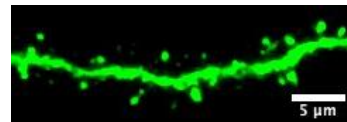
J. Apical 1



K. Apical 2

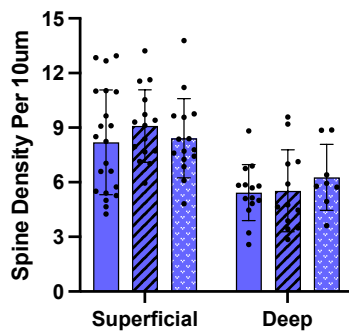


L. Basilar

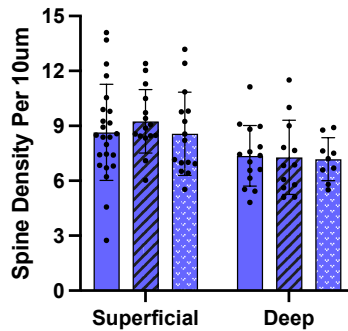


M.

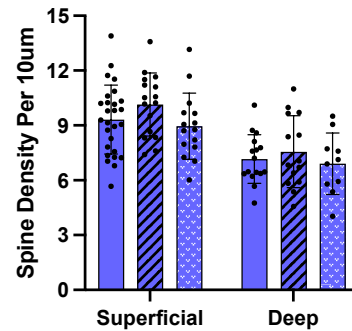
Contra S1FL Primary Apical



Contra S1FL Secondary Apical



Contra S1FL Basilar



□ = Sham (N=9)

▨ = Stroke+1 Week (N=6)

▤ = Stroke+6 Weeks (N=5)

● = 1 Neuron

Figure 11: Within Contra-S1FL, no changes in dendritic spine density 1-week or 6-weeks after stroke

A-C. Retrogradely labelled neurons in Contra-S1FL region in both superficial and deep cortical depths within the sham group. **D-F.** Enlarged image of Contra-S1FL primary apical, secondary apical and basilar dendrite within the sham group. **G-I.** Retrogradely labelled neurons in Contra-Peri-infarct region in both superficial and deep cortical depths after stroke. **J-L.** Enlarged image of Contra-Peri-infarct primary apical, secondary apical and basilar dendrites 1-week after stroke. **M-O.** In primary apical, secondary apical, and basilar dendrites within Contra-S1FL/Peri-infarct, no changes in spine density were observed in superficial or deep layers 1-week or 6-weeks after stroke. Error bars: mean±SD.

Table 1: Two-way ANOVA of primary apical spine density with Depth (superficial vs deep) and Experimental Group (sham vs 1-week stroke vs 6-week stroke) as factors

Area	Depth	Stroke	Interaction
S1FL	F (1, 83) = 20.24, p<0.0001	F (2, 83) = 5.641, p=0.0050	F (2, 83) = 0.9330, p=0.3974
Motor	F (1, 83) = 12.70, p=0.0006	F (2, 83) = 4.387, p=0.0154	F (2, 83) = 2.155, p=0.1223
S2	F (1, 87) = 68.60, p<0.0001	F (2, 87) = 4.540, p=0.0133	F (2, 87) = 1.485, p=0.2321
Contra S1FL	F (1, 79) = 31.07, p<0.0001	F (2, 79) = 0.5159, p=0.5990	F (2, 79) = 0.5963, p=0.5533

Table 2: Two-way ANOVA of secondary apical spine density with Depth (superficial vs deep) and Experimental Group (sham vs 1-week stroke vs 6-week stroke) as factors. Significant main effects are highlighted in bold.

Area	Depth	Stroke	Interaction
S1FL	F (1, 89) = 9.611, p=0.0026	F (2, 89) = 1.919, p=0.1528	F (2, 89) = 0.03249, p=0.9680
Motor	F (1, 90) = 1.190, p=0.2783	F (2, 90) = 2.534, p=0.0850	F (2, 90) = 0.1792, p=0.8362
S2	F (1, 92) = 5.886, p=0.0172	F (2, 92) = 8.019, p=0.0006	F (2, 92) = 0.5821, p=0.5608
Contra S1FL	F (1, 84) = 11.30, p=0.0012	F (2, 84) = 0.2260, p=0.7982	F (2, 84) = 0.2213, p=0.8019

Table 3: Two-way ANOVA of basilar spine density with Depth (superficial vs deep) and Experimental Group (sham vs 1-week stroke vs 6-week stroke) as factors. Significant main effects are highlighted in bold.

Area	Depth	Stroke	Interaction
S1FL	F (1, 94) = 38.10, p<0.0001	F (2, 94) = 8.581, p=0.0004	F (2, 94) = 0.4125, p=0.6632
Motor	F (1, 95) = 13.81, p=0.0003	F (2, 95) = 2.061, p=0.1330	F (2, 95) = 0.6950, p=0.5016
S2	F (1, 94) = 33.04, p<0.0001	F (2, 94) = 7.232, p=0.0012	F (2, 94) = 0.01487, p=0.9852
Contra S1FL	F (1, 92) = 37.19, p<0.0001	F (2, 92) = 1.974, p=0.1448	F (2, 92) = 0.1806, p=0.8351

3.6 Decrease 1-week after stroke in peri-infarct spines cannot be explained by the branching direction of the dendrite, size of the infarct or distance to the infarct

Further investigation was conducted to determine factors that could be influencing the decrease in superficial basilar dendritic spines seen 1-week after stroke in the peri-infarct (as shown highlighted in purple in the schematic image in Figure 12A). First, we wanted to know if the superficial basilar dendrites that were affected were specific to dendrites projecting towards the stroke site. To determine this, I analyzed spine density in superficial basilar dendrites either projecting towards or away from the infarct. Analysis revealed no significant differences between the two groups (Figure 12B; $t(36)=1.358$, $p=0.1828$).

Next, we were curious if the size of the stroke had an impact on spine density within the peri-infarct. This was measured using a simple linear regression for primary apical, secondary apical and basilar dendrites, which revealed no significant effect of infarct size (Figure 12C=primary apical: $r^2=0.008117$, $p=0.6616$; Figure 12D=secondary apical: $r^2=1.927e-006$, $p=0.9944$; Figure 12E=basilar: $r^2=0.006877$, $p=0.6631$).

Lastly, it was hypothesized that the distance a neuron was from the infarct may play a role in spine density changes. This was measured using a simple linear regression for primary apical, secondary apical and basilar dendrites, which revealed no significant effect of distance (Figure 12F=primary apical: $r^2=0.08941$, $p=0.1378$; Figure 12G=secondary apical: $r^2=0.09831$, $p=0.0977$; Figure 12H=basilar: $r^2=0.02385$, $p=0.4152$).

Overall, these analyses suggest that the loss of basilar dendritic spines in peri-infarct neurons after stroke is not due to the branching direction of the dendrite, the size of the stroke, or the distance of the neuron from the infarct.

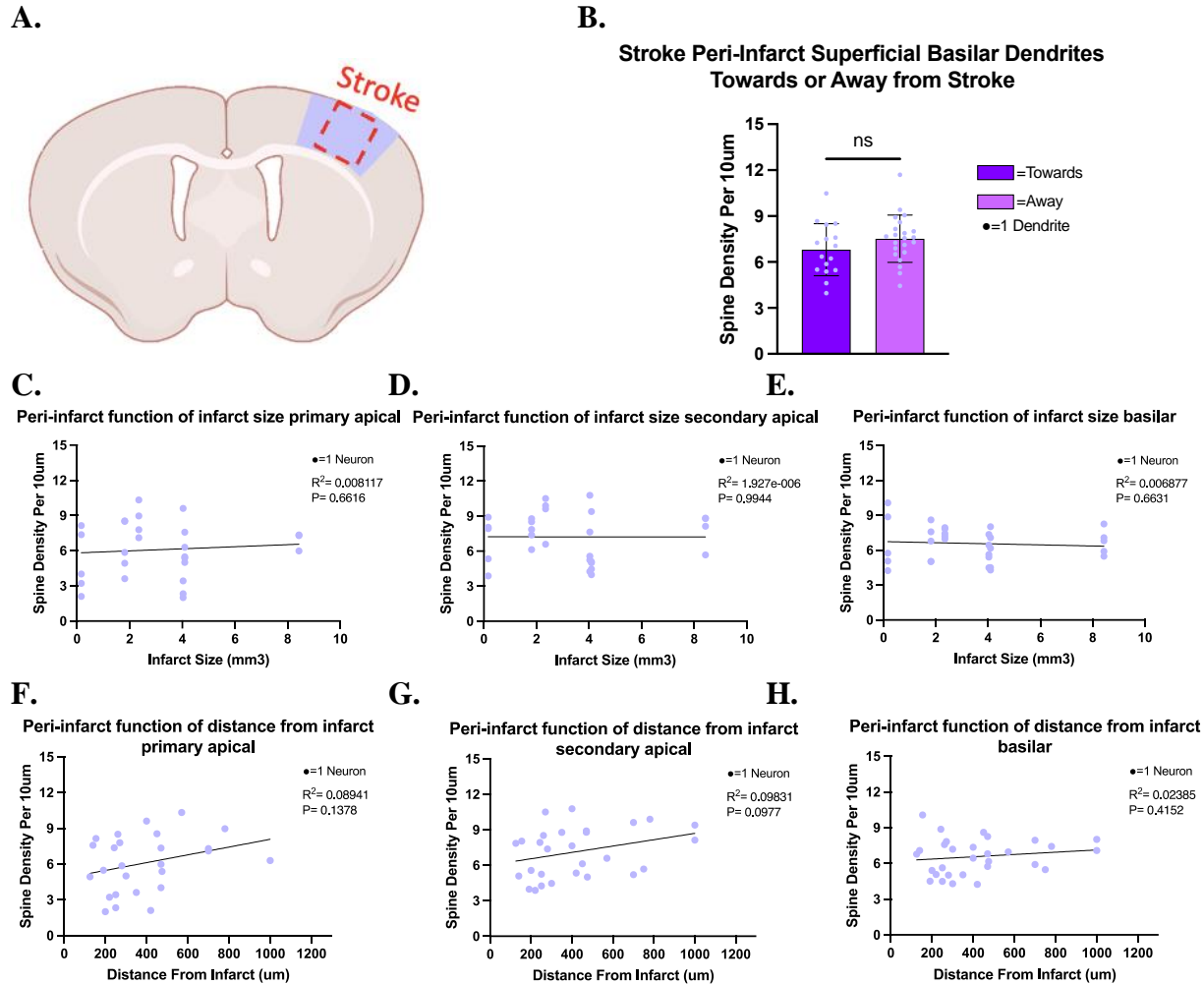


Figure 12: Spine density reduction in peri-infarct basilar dendrites 1-week after stroke is not affected by branching direction of the dendrite, size of the infarct or distance to the infarct

A. Schematic representation of the peri-infarct region, which is investigated further in the following graphs. **B.** 1-week after stroke (n=6), no significant difference was found within the peri-infarct when comparing superficial basilar dendrites projecting towards or away from the stroke site. **C-E.** Dendritic spine density did not differ 1-week after stroke in the peri-infarct as a function of infarct size within primary apical dendrites (C), secondary apical dendrites (D) or basilar dendrites (E). **F-H.** Dendritic spine density did not differ 1-week after stroke in the peri-infarct as a function of distance from the infarct within primary apical dendrites (E), secondary apical dendrites (F) or basilar dendrites (G). Error bars: mean±SD.

4. Discussion

4.1 Overview

It is well established that dendritic spines play a crucial role in plasticity and recovery post-stroke, and since they are sensitive to injury it becomes important to further elucidate specific structural changes to spines throughout the cortex. The brain connectome is a vast system of neural networks that can be hindered or help to compensate for functional deficits after injury. This neural circuitry is connected by synapses which are located at dendritic spines. There is a gap in the literature when studying the impacts of ischemia on dendritic spines on neurons that are directly connected to the stroke site throughout the brain. Using neural tracing and confocal microscopy, we were able to label presynaptic neurons projecting to the infarct site from the peri-infarct and distant regions and quantify dendritic spine densities at two-time points; 1- and 6-week post-stroke.

The first area of research that calls for discussion is the investigation of sex differences after stroke in selected regions throughout the connectome. Many previous research studies investigating dendritic spines after stroke did not investigate or report sex differences (Ito et al., 2006; Papadopoulos et al., 2006; Enright et al., 2007; Brown et al., 2008; Johnston et al., 2013; Huang et al., 2018; Tu et al., 2022; Merino-Serrais et al., 2023). Although my results found no significant sex differences in spine density in sham- or stroke-group throughout the brain, this area of research needs to be examined more in the future with sufficient sampling in order to make confident conclusions.

The second finding from this research study was higher dendritic spine densities within secondary apical dendrites compared to primary, whereas no effect of branch order was found in basilar dendrites. Similarly, a previous study looked at pyramidal neurons from layer 3 of S1 and

found that main apical dendrites had less spines than apical collateral dendrites, and that apical collateral and basilar dendrites had similar values (Merino-Serrais et al., 2023). These findings corroborate the results found in my research.

Next, we reported on spine density in neurons within different cortical depths throughout the brain. Our results revealed significantly higher spine densities in superficial cortical neurons compared to deep cortical neurons in many of the brain regions. Other research has found similar findings of higher spine densities in apical dendrites of layer 2/3 pyramidal neurons compared to layer 5 (Tjia et al., 2017), higher spine densities in apical dendrites of layer 2 pyramidal neurons (Hutsler & Zhang, 2010), and higher spine densities in superficial pyramidal neurons compared to deep pyramidal neurons (Masurkar et al., 2017).

The main objective of this research study was to investigate dendritic spine density 1-week and 6-weeks after stroke, throughout the connectome. The results revealed that only peri-infarct superficial basilar dendrites exhibited a decrease in spines 1-week after stroke. Previous research has similarly found that spine density is not impacted after stroke in more distant brain regions (Papadopoulos et al., 2006; Enright et al., 2007; Brown et al., 2008; Johnston et al., 2013; Tu et al., 2022; Merino-Serrais et al., 2023). This loss in basilar dendritic spines specifically within the peri-infarct may be attributed to a few factors, such as deafferentation, inflammation/pro-inflammatory microglia and spreading depolarizations/hypo-excitability. Deafferentation occurs when there is a loss of sensory input and can therefore lead to neural adaptations. It has been shown in literature that deafferentations can result in changes in dendritic structure, such as the loss of spines (Jones & Thomas, 1962; Butz et al., 2009; Mostany et al., 2010; Dorostkar et al., 2015). When neurons are destroyed in the infarct core, the neurons projecting to this region lose their post-synaptic connection, which may influence the excitability of the neuron and therefore the

number of synapses on the presynaptic neuron. Although this would help to explain a decrease in retrograde spines after stroke, it does not explain why this is limited to the peri-infarct region. Another mechanism that impacts dendritic spines after stroke is microglia. It is well established that microglia respond quickly to stroke (Y. Zhang et al., 2022), and have an impact on the structure and function of surrounding neurons. Pro-inflammatory microglia release cytokines such as tumor-necrosis factor alpha (TNF- α) and interleukin-1 beta (IL-1 β) which increase inflammation and injury to the tissue (Kanazawa et al., 2017; Y. Zhang et al., 2022) and are well-characterized in stroke. These cytokines can exacerbate pro-inflammatory processes, which include modification and the loss or “eating” of dendritic spines (Prada et al., 2018; Y. Zhang et al., 2022; Haupt et al., 2024). It is possible that there are high volumes of pro-inflammatory microglia close to the site of injury, resulting in the reduction of spines in the peri-infarct that is not seen in more distant regions outside the zone of inflammation.

Moreover, when discussing the impact of stroke on neurons, spreading depolarizations and the consequential hypo-excitability may also play a role on spine density after stroke. Spreading depolarizations that occur acutely after stroke have been shown to result in loss of dendritic structure and spines (Takano et al., 2007; Murphy et al., 2008; Risher et al., 2010). These waves also induce inflammatory cascades (Chung et al., 2016), which could lead to increased pro-inflammatory microglia responses. After stroke induced depolarizations, there is a period of hypo-excitability (Carmichael, 2012) where the neural activity is reduced. This reduction in neural activity may coincide with a reduced number of spines, as there may be less synaptic activity. The impact of spreading depolarization on neurons varies depending on distance to the infarct core (Strong et al., 2006), which could help to explain why we see this loss in spines specifically in the peri-infarct and not in distant regions. A question that has not been answered is why the loss in the

peri-infarct region is specific to superficial basilar dendrites. One factor that may be contributing to this specific decrease in spine density, is that superficial cortical layers make significantly more inter-regional lateral connections (Douglas & Martin, 2004). Basilar dendrites also contribute vastly to inter-regional lateral connections; therefore, the basilar dendrites of superficial peri-infarct neurons may be losing the neurons they project to, which are damaged by the stroke.

When looking at the recovery of dendritic spines after stroke, we saw spine density return to baseline in superficial basilar dendrites in the peri-infarct, as well as increase in other peri-infarct and S2 dendrites 6-weeks after stroke. The stability of dendritic spines throughout the brain connectome, the recovery of spines within the peri-infarct region and the increase in spines 6-weeks after stroke can be explained by a multitude of factors such as reperfusion, anti-inflammatory microglia, and neuroplasticity. Reperfusion after stroke may play a significant role in the loss and recovery of spines after stroke. Research has shown that distant regions with more preserved blood flow may recover faster and lead to increased spines (Mostany et al., 2010), which could help explain stable, and even at times increased spine densities after stroke in regions further from the infarct. This may also help to explain recovery within the peri-infarct itself, as perfusion may still be impacted 1-week after stroke but fully recover 6-weeks after stroke. Another factor that impacts the recovery of spines after stroke is microglia. Not only do they play a pro-inflammatory role, but they have anti-inflammatory influences. These defense and repair mechanisms can play a large role in maintaining brain homeostasis (Y. Zhang et al., 2022). Anti-inflammatory cytokines released by microglia such as transforming growth factor beta (TGF- β), IL-4 and IL-10 and growth factors such as vascular endothelial growth factor (VEGF) and brain-derived neurotrophic factor (BDNF) can reduce inflammation and assist in recovery (Kanazawa et al., 2017). These cytokines and growth factors can alter structures such as dendritic spines to help

recovery (Haupt et al., 2024). Microglia have also been shown to play a role in synaptogenesis, in which they can cause intracellular calcium release within the neuron resulting in higher chances of synapse formation (Eldahshan et al., 2019; Blagburn-Blanco et al., 2022; Wang et al., 2022; Y. Zhang et al., 2022). It is possible that more distant brain regions from the infarct may experience higher amounts of anti-inflammatory microglia to promote recovery and maintain the brain's homeostasis. These anti-inflammatory microglia may also play a role in the recovery we see 6-weeks after stroke in the peri-infarct once the pro-inflammatory mechanisms have subsided.

A mechanism that may likely be influencing the stability, recovery and increase in spines in the connectome is neuroplasticity. Structural neuroplasticity takes many forms, such as axonal sprouting and the formation of new neural connections, both of which are associated with recovery (Stroemer et al., 1995; Carmichael et al., 2001; Dancause et al., 2005; Murphy & Corbett, 2009; S. Li et al., 2010; Overman et al., 2012). Changes in dendritic spine structure is a common homeostatic process after stroke that can help return synaptic activity to normal, and therefore be a marker of structural plasticity (Brown et al., 2007, 2008, 2009, 2010; Murphy & Corbett, 2009; Mostany et al., 2010; Gerrow & Brown, 2017). This neuroplasticity that is shown by axonal sprouting and changes in dendritic spines may be a reason as to why distant brain regions are more resilient after stroke, and why we see later recovery of spines in the peri-infarct. The main mechanism that may be contributing to the increase in spine density 6-weeks after stroke in the peri-infarct and S2 is neuroplasticity acting as a compensation mechanism. This compensation seems to be primarily acting in the region of damage as well as functionally associated areas. Functional plasticity has been shown to recruit neighboring regions following stroke (Winship & Murphy, 2008; Brown et al., 2009). The functional mapping near the infarct may occur due to structural changes that influence synapse formation and circuit reorganization (Gerrow & Brown,

2017; Campos et al., 2023). This functional remapping could explain why we see an increase in spine density within the ipsilateral S2 6-weeks after stroke, as this nearby functionally associated region may be recruited as a form of plasticity. Other research has stated that stroke leads to the excitability in neuronal circuits adjacent to the infarct, which may be underlying the brain remapping and recovery (Carmichael, 2012). This increased excitability in regions near the infarct such as the peri-infarct and S2 could explain this compensatory increase in spines 6-weeks after stroke.

4.2 Limitations

Although this study contributed valuable information about structural changes throughout the connectome after stroke, there are limitations that need to be discussed. Firstly, the retrograde virus was variable in its labelling throughout the cortex, which resulted in needing more mice to get sufficient sampling. Although it is important to look at how presynaptic neurons are impacted throughout the brain, there may be a different type of retrograde AAV that would be more consistent in its labeling, which would permit for less animal use.

Second, this study was conducted *ex vivo* because we were looking at multiple brain regions, which would not have been conceivable to do *in vivo* as a cranial window only allows for the imaging of a small area. This means that we can only make correlations about comparisons between shams, 1- and 6-week stroke groups, rather than seeing it in the same mice over time. Similarly, we only looked at two time points after stroke: 1- and 6-weeks. This allows us to make assumptions about acute and chronic changes after stroke, however we are limited in our knowledge about what is happening to retrograde spine density between those timepoints, and initially after stroke. Previous research has found retrograde degeneration 24 hours after stroke

that impacts spine density (Nagendran et al., 2017), therefore this may be an interesting time point to study.

Lastly, this study did not investigate functional changes due to time constriction. Behavioural studies in addition to studying spine density would have allowed for a better understanding of the functional implications to the structural changes we saw throughout the connectome after stroke. Therefore, behavioural tests would make our data more translatable for clinical applications.

4.3 Future Directions

Due to the complexity of the brain and its mechanisms after stroke, there are still many questions that need to be answered about structural modifications throughout the connectome. The first future direction I would like to discuss is in relation to my own research, which involves increasing the sample size to confidently conclude whether there are differences seen after stroke in MC. As reported in the results, the ANOVA showed a significant main effect of stroke in primary apical dendrites within MC, and although close, the multiple comparisons did not reveal significance. This causes some concern due to the variability in my data. Increasing the sample size will help to confidently conclude whether there are retrograde changes seen within MC and provide large implications for connectomic plasticity and future research.

Future research may also want to increase sample size to properly investigate sex differences, as this study was too undersampled to do so. Although non-significant, interesting results were seen within females 1-week after stroke in which they had higher spine density than males in the contralateral hemisphere, potentially revealing sex-dependent compensation mechanisms. This is consistent with other research showing females have more interhemispheric connectivity (Ingalhalikar et al., 2014; Tyan et al., 2017; Bonelli et al., 2022). Future studies may

want to research this further to determine whether spine density may be a structural marker of this interhemispheric connectivity in females.

Lastly, future research may want to investigate functional changes in sensorimotor behaviour in tandem with looking at spine density in the connectome. For example, we can measure both ipsilateral and contralateral sensorimotor functioning using metrics such as the ladder, tape and cylinder test. As mentioned in the limitation section, this would provide more translatable information for clinical applications, and help to fully understand how structural changes after stroke throughout the brain may be impacting behaviour and function.

5. Conclusion

This thesis aimed to investigate changes in dendritic spine density in neurons projecting to the stroke site throughout the brain connectome. This was due to a gap in the literature when studying dendritic spine density in directly connected neurons to the stroke site, in multiple different brain regions. By utilizing confocal microscopy, I was able to image neurons projecting to the stroke site in four different brain regions: S1FL, MC, S2 and Contra-S1FL. The results revealed that a decrease in dendritic spine density 1-week after stroke was specific to superficial basilar dendrites in the peri-infarct region, which recovered 6-weeks after stroke. This decrease in density did not extend to more distal brain regions, which shows that a retrograde degenerative signal that impacts dendritic spines may be localized to near the infarct site. On the other hand, we saw an increase in dendritic spine density within the peri-infarct region and S2 6-weeks after stroke. This reveals that structural plasticity within the neural connections throughout the connectome may be playing a role in stroke recovery. In conclusion, these findings provide novel information about retrograde signaling in neurons directly connected to the infarct core throughout the brain, as well as elucidate potential degenerative and protective structural processes that could underly function after stroke.

References

- Andrew, R. D., Hartings, J. A., Ayata, C., Brennan, K. C., Dawson-Scully, K. D., Farkas, E., Herreras, O., Kirov, S. A., Müller, M., Ollen-Bittle, N., Reiffurth, C., Revah, O., Robertson, R. M., Shuttleworth, C. W., Ullah, G., & Dreier, J. P. (2022). The Critical Role of Spreading Depolarizations in Early Brain Injury: Consensus and Contention. *Neurocritical Care*, 37(Suppl 1), 83–101. <https://doi.org/10.1007/s12028-021-01431-w>
- Araya, R. (2014). Input transformation by dendritic spines of pyramidal neurons. *Frontiers in Neuroanatomy*, 8. <https://www.frontiersin.org/journals/neuroanatomy/articles/10.3389/fnana.2014.00141>
- Betley, J. N., & Sternson, S. M. (2011). Adeno-associated viral vectors for mapping, monitoring, and manipulating neural circuits. *Human Gene Therapy*, 22(6), 669–677. <https://doi.org/10.1089/hum.2010.204>
- Bhatt, D. H., Zhang, S., & Gan, W.-B. (2009). Dendritic Spine Dynamics. In *Annual Review of Physiology* (Vol. 71, Issue Volume 71, 2009, pp. 261–282). Annual Reviews. <https://doi.org/10.1146/annurev.physiol.010908.163140>
- Blagburn-Blanco, S. V., Chappell, M. S., De Biase, L. M., & DeNardo, L. A. (2022). Synapse-specific roles for microglia in development: New horizons in the prefrontal cortex. *Frontiers in Molecular Neuroscience*, 15, 965756. <https://doi.org/10.3389/fnmol.2022.965756>
- Boehme, A. K., Esenwa, C., & Elkind, M. S. V. (2017). Stroke Risk Factors, Genetics, and Prevention. *Circulation Research*, 120(3), 472–495. <https://doi.org/10.1161/CIRCRESAHA.116.308398>

- Bonelli, C., Mancuso, L., Manuello, J., Liloia, D., Costa, T., & Cauda, F. (2022). Sex differences in brain homotopic co-activations: A meta-analytic study. *Brain Structure & Function*, 227(8), 2839–2855. <https://doi.org/10.1007/s00429-022-02572-0>
- Branco, J. P., Oliveira, S., Sargento-Freitas, J., Laíns, J., & Pinheiro, J. (2019). Assessing functional recovery in the first six months after acute ischemic stroke: A prospective, observational study. *European Journal of Physical and Rehabilitation Medicine*, 55(1), 1–7. <https://doi.org/10.23736/S1973-9087.18.05161-4>
- Brown, C. E., Aminoltejari, K., Erb, H., Winship, I. R., & Murphy, T. H. (2009). *In Vivo* Voltage-Sensitive Dye Imaging in Adult Mice Reveals That Somatosensory Maps Lost to Stroke Are Replaced over Weeks by New Structural and Functional Circuits with Prolonged Modes of Activation within Both the Peri-Infarct Zone and Distant Sites. *The Journal of Neuroscience*, 29(6), 1719–1734. <https://doi.org/10.1523/JNEUROSCI.4249-08.2009>
- Brown, C. E., Boyd, J. D., & Murphy, T. H. (2010). Longitudinal *in vivo* Imaging Reveals Balanced and Branch-Specific Remodeling of Mature Cortical Pyramidal Dendritic Arbors after Stroke. *Journal of Cerebral Blood Flow & Metabolism*, 30(4), 783–791. <https://doi.org/10.1038/jcbfm.2009.241>
- Brown, C. E., Li, P., Boyd, J. D., Delaney, K. R., & Murphy, T. H. (2007). Extensive Turnover of Dendritic Spines and Vascular Remodeling in Cortical Tissues Recovering from Stroke. *The Journal of Neuroscience*, 27(15), 4101–4109. <https://doi.org/10.1523/JNEUROSCI.4295-06.2007>

- Brown, C. E., Wong, C., & Murphy, T. H. (2008). Rapid Morphologic Plasticity of Peri-Infarct Dendritic Spines After Focal Ischemic Stroke. *Stroke*, *39*(4), 1286–1291.
<https://doi.org/10.1161/STROKEAHA.107.498238>
- Butz, M., Van Ooyen, A., & Wörgötter, F. (2009). A model for cortical rewiring following deafferentation and focal stroke. *Frontiers in Computational Neuroscience*, *3*.
<https://www.frontiersin.org/journals/computational-neuroscience/articles/10.3389/neuro.10.010.2009>
- Callaway, E. M. (2005). A molecular and genetic arsenal for systems neuroscience. *Trends in Neurosciences*, *28*(4), 196–201. <https://doi.org/10.1016/j.tins.2005.01.007>
- Campbell, B. C. V., De Silva, D. A., Macleod, M. R., Coutts, S. B., Schwamm, L. H., Davis, S. M., & Donnan, G. A. (2019). Ischaemic stroke. *Nature Reviews Disease Primers*, *5*(1), 70. <https://doi.org/10.1038/s41572-019-0118-8>
- Campos, B., Choi, H., DeMarco, A. T., Seydell-Greenwald, A., Hussain, S. J., Joy, M. T., Turkeltaub, P. E., & Zeiger, W. (2023). Rethinking Remapping: Circuit Mechanisms of Recovery after Stroke. *The Journal of Neuroscience*, *43*(45), 7489–7500.
<https://doi.org/10.1523/JNEUROSCI.1425-23.2023>
- Carmichael, S. T. (2005). Rodent models of focal stroke: Size, mechanism, and purpose. *NeuroRX*, *2*(3), 396–409. <https://doi.org/10.1602/neurorx.2.3.396>
- Carmichael, S. T. (2006). Cellular and molecular mechanisms of neural repair after stroke: Making waves. *Annals of Neurology*, *59*(5), 735–742. <https://doi.org/10.1002/ana.20845>
- Carmichael, S. T. (2012). Brain Excitability in Stroke: The Yin and Yang of Stroke Progression. *Archives of Neurology*, *69*(2), 161. <https://doi.org/10.1001/archneurol.2011.1175>

- Carmichael, S. T., Tatsukawa, K., Katsman, D., Tsuyuguchi, N., & Kornblum, H. I. (2004). Evolution of Diaschisis in a Focal Stroke Model. *Stroke*, *35*(3), 758–763.
<https://doi.org/10.1161/01.STR.0000117235.11156.55>
- Carmichael, S. T., Wei, L., Rovainen, C. M., & Woolsey, T. A. (2001). New patterns of intracortical projections after focal cortical stroke. *Neurobiology of Disease*, *8*(5), 910–922. <https://doi.org/10.1006/nbdi.2001.0425>
- Carrera, E., & Tononi, G. (2014). Diaschisis: Past, present, future. *Brain*, *137*(9), 2408–2422.
<https://doi.org/10.1093/brain/awu101>
- Carter, A. R., Shulman, G. L., & Corbetta, M. (2012). Why use a connectivity-based approach to study stroke and recovery of function? *NeuroImage*, *62*(4), 2271–2280.
<https://doi.org/10.1016/j.neuroimage.2012.02.070>
- Castro-Alamancos, M. A., & Borrell, J. (1995). Functional recovery of forelimb response capacity after forelimb primary motor cortex damage in the rat is due to the reorganization of adjacent areas of cortex. *Neuroscience*, *68*(3), 793–805.
[https://doi.org/10.1016/0306-4522\(95\)00178-L](https://doi.org/10.1016/0306-4522(95)00178-L)
- Chugh, C. (2019). Acute Ischemic Stroke: Management Approach. *Indian Journal of Critical Care Medicine: Peer-Reviewed, Official Publication of Indian Society of Critical Care Medicine*, *23*(Suppl 2), S140–S146. <https://doi.org/10.5005/jp-journals-10071-23192>
- Chung, D. Y., Oka, F., & Ayata, C. (2016). Spreading Depolarizations: A Therapeutic Target Against Delayed Cerebral Ischemia After Subarachnoid Hemorrhage. *Journal of Clinical Neurophysiology: Official Publication of the American Electroencephalographic Society*, *33*(3), 196–202. <https://doi.org/10.1097/WNP.0000000000000275>

- Connell, L., Lincoln, N., & Radford, K. (2008). Somatosensory impairment after stroke: Frequency of different deficits and their recovery. *Clinical Rehabilitation*, 22(8), 758–767. <https://doi.org/10.1177/0269215508090674>
- Corbett, D., Giles, T., Evans, S., McLean, J., & Biernaskie, J. (2006). Dynamic changes in CA1 dendritic spines associated with ischemic tolerance. *Experimental Neurology*, 202(1), 133–138. <https://doi.org/10.1016/j.expneurol.2006.05.020>
- Cramer, S. C., Richards, L. G., Bernhardt, J., & Duncan, P. (2023). Cognitive Deficits After Stroke. *Stroke*, 54(1), 5–9. <https://doi.org/10.1161/STROKEAHA.122.041775>
- Dancause, N., Barbay, S., Frost, S. B., Plautz, E. J., Chen, D., Zoubina, E. V., Stowe, A. M., & Nudo, R. J. (2005). Extensive Cortical Rewiring after Brain Injury. *The Journal of Neuroscience*, 25(44), 10167–10179. <https://doi.org/10.1523/JNEUROSCI.3256-05.2005>
- Deutch, A. Y., Colbran, R. J., & Winder, D. J. (2007). Striatal plasticity and medium spiny neuron dendritic remodeling in parkinsonism. *Proceedings of the XVII WFN World Congress on Parkinson's Disease and Related Disorders*, 13, S251–S258. [https://doi.org/10.1016/S1353-8020\(08\)70012-9](https://doi.org/10.1016/S1353-8020(08)70012-9)
- Dijkhuizen, R. M., Ren, J., Mandeville, J. B., Wu, O., Ozdag, F. M., Moskowitz, M. A., Rosen, B. R., & Finklestein, S. P. (2001). Functional magnetic resonance imaging of reorganization in rat brain after stroke. *Proceedings of the National Academy of Sciences of the United States of America*, 98(22), 12766–12771. <https://doi.org/10.1073/pnas.231235598>
- Dorostkar, M. M., Zou, C., Blazquez-Llorca, L., & Herms, J. (2015). Analyzing dendritic spine pathology in Alzheimer's disease: Problems and opportunities. *Acta Neuropathologica*, 130(1), 1–19. <https://doi.org/10.1007/s00401-015-1449-5>

- Douglas, R. J., & Martin, K. A. C. (2004). Neuronal circuits of the neocortex. *Annual Review of Neuroscience*, 27, 419–451. <https://doi.org/10.1146/annurev.neuro.27.070203.144152>
- Eldahshan, W., Fagan, S. C., & Ergul, A. (2019). Inflammation within the neurovascular unit: Focus on microglia for stroke injury and recovery. *Pharmacological Research*, 147, 104349. <https://doi.org/10.1016/j.phrs.2019.104349>
- Empl, L., Chovsepian, A., Chahin, M., Kan, W. Y. V., Fourneau, J., Van Steenberghe, V., Weidinger, S., Marcantoni, M., Ghanem, A., Bradley, P., Conzelmann, K. K., Cai, R., Ghasemigharagoz, A., Ertürk, A., Wagner, I., Kreutzfeldt, M., Merkler, D., Liebscher, S., & Bareyre, F. M. (2022). Selective plasticity of callosal neurons in the adult contralesional cortex following murine traumatic brain injury. *Nature Communications*, 13(1), 2659. <https://doi.org/10.1038/s41467-022-29992-0>
- Enright, L. E., Zhang, S., & Murphy, T. H. (2007). Fine mapping of the spatial relationship between acute ischemia and dendritic structure indicates selective vulnerability of layer V neuron dendritic tufts within single neurons in vivo. *Journal of Cerebral Blood Flow and Metabolism: Official Journal of the International Society of Cerebral Blood Flow and Metabolism*, 27(6), 1185–1200. <https://doi.org/10.1038/sj.jcbfm.9600428>
- Feigin, V. L., Brainin, M., Norrving, B., Martins, S., Sacco, R. L., Hacke, W., Fisher, M., Pandian, J., & Lindsay, P. (2022). World Stroke Organization (WSO): Global Stroke Fact Sheet 2022. *International Journal of Stroke*, 17(1), 18–29. <https://doi.org/10.1177/17474930211065917>
- Finger, S., Koehler, P. J., & Jagella, C. (2004). The Monakow Concept of Diaschisis: Origins and Perspectives. *Archives of Neurology*, 61(2), 283–288. <https://doi.org/10.1001/archneur.61.2.283>

- Florence, S. L., Taub, H. B., & Kaas, J. H. (1998). Large-Scale Sprouting of Cortical Connections After Peripheral Injury in Adult Macaque Monkeys. *Science*, 282(5391), 1117–1121. <https://doi.org/10.1126/science.282.5391.1117>
- Gao, X., Deng, P., Xu, Z. C., & Chen, J. (2011). Moderate Traumatic Brain Injury Causes Acute Dendritic and Synaptic Degeneration in the Hippocampal Dentate Gyrus. *PLoS ONE*, 6(9), e24566. <https://doi.org/10.1371/journal.pone.0024566>
- Gemin, O., Serna, P., Zamith, J., Assendorp, N., Fossati, M., Rostaing, P., Triller, A., & Charrier, C. (2021). Unique properties of dually innervated dendritic spines in pyramidal neurons of the somatosensory cortex uncovered by 3D correlative light and electron microscopy. *PLOS Biology*, 19(8), e3001375. <https://doi.org/10.1371/journal.pbio.3001375>
- George Paxinos & Keither Franklin. (2004). *The Mouse Brain in Stereotaxic Coordinates* (2nd ed.). Elsevier Science.
- Gerrow, K., & Brown, C. E. (2017). Chapter 3—Structural Neural Plasticity During Stroke Recovery**This work was supported by operating, salary, and equipment grants to C.E.B. from CIHR, Heart and Stroke Foundation of BC and Yukon, MSFHR, NSERC, and CFI. In A. van Ooyen & M. Butz-Ostendorf (Eds.), *The Rewiring Brain* (pp. 49–70). Academic Press. <https://doi.org/10.1016/B978-0-12-803784-3.00003-2>
- Ghosh, A., Peduzzi, S., Snyder, M., Schneider, R., Starkey, M., & Schwab, M. E. (2012). Heterogeneous Spine Loss in Layer 5 Cortical Neurons after Spinal Cord Injury. *Cerebral Cortex*, 22(6), 1309–1317. <https://doi.org/10.1093/cercor/bhr191>

- Gipson, C. D., & Olive, M. F. (2017). Structural and functional plasticity of dendritic spines—
Root or result of behavior? *Genes, Brain, and Behavior*, *16*(1), 101–117.
<https://doi.org/10.1111/gbb.12324>
- Gonzalez, C. L. R., & Kolb, B. (2003). A comparison of different models of stroke on behaviour
and brain morphology. *European Journal of Neuroscience*, *18*(7), 1950–1962.
<https://doi.org/10.1046/j.1460-9568.2003.02928.x>
- Grutzendler, J., Kasthuri, N., & Gan, W.-B. (2002). Long-term dendritic spine stability in the
adult cortex. *Nature*, *420*(6917), 812–816. <https://doi.org/10.1038/nature01276>
- Gülke, E., Gelderblom, M., & Magnus, T. (2018). Danger signals in stroke and their role on
microglia activation after ischemia. *Therapeutic Advances in Neurological Disorders*, *11*,
175628641877425. <https://doi.org/10.1177/1756286418774254>
- Harris, K. M. (1999). Structure, development, and plasticity of dendritic spines. *Current Opinion
in Neurobiology*, *9*(3), 343–348. [https://doi.org/10.1016/s0959-4388\(99\)80050-6](https://doi.org/10.1016/s0959-4388(99)80050-6)
- Haupt, M., Gerner, S. T., & Doeppner, T. R. (2024). The dual role of microglia in ischemic
stroke and its modulation via extracellular vesicles and stem cells. *Neuroprotection*, *2*(1),
4–15. <https://doi.org/10.1002/nep3.39>
- He, F., Sullender, C. T., Zhu, H., Williamson, M. R., Li, X., Zhao, Z., Jones, T. A., Xie, C.,
Dunn, A. K., & Luan, L. (2020). Multimodal mapping of neural activity and cerebral
blood flow reveals long-lasting neurovascular dissociations after small-scale strokes.
Science Advances, *6*(21), eaba1933. <https://doi.org/10.1126/sciadv.aba1933>
- Hermann, D. M., & Chopp, M. (2012). Promoting brain remodelling and plasticity for stroke
recovery: Therapeutic promise and potential pitfalls of clinical translation. *The Lancet.
Neurology*, *11*(4), 369–380. [https://doi.org/10.1016/S1474-4422\(12\)70039-X](https://doi.org/10.1016/S1474-4422(12)70039-X)

- Holtmaat, A., Wilbrecht, L., Knott, G. W., Welker, E., & Svoboda, K. (2006). Experience-dependent and cell-type-specific spine growth in the neocortex. *Nature*, *441*(7096), 979–983. <https://doi.org/10.1038/nature04783>
- Huang, S.-Y., Chang, C.-H., Hung, H.-Y., Lin, Y.-W., & Lee, E.-J. (2018). Neuroanatomical and electrophysiological recovery in the contralateral intact cortex following transient focal cerebral ischemia in rats. *Neurological Research*, *40*(2), 130–138. <https://doi.org/10.1080/01616412.2017.1411454>
- Hui, C., Tadi, P., Khan Suheb, M. Z., & Patti, L. (2024). Ischemic Stroke. In *StatPearls*. StatPearls Publishing. <http://www.ncbi.nlm.nih.gov/books/NBK499997/>
- Hutsler, J. J., & Zhang, H. (2010). Increased dendritic spine densities on cortical projection neurons in autism spectrum disorders. *Brain Research*, *1309*, 83–94. <https://doi.org/10.1016/j.brainres.2009.09.120>
- Ingalhalikar, M., Smith, A., Parker, D., Satterthwaite, T. D., Elliott, M. A., Ruparel, K., Hakonarson, H., Gur, R. E., Gur, R. C., & Verma, R. (2014). Sex differences in the structural connectome of the human brain. *Proceedings of the National Academy of Sciences of the United States of America*, *111*(2), 823–828. <https://doi.org/10.1073/pnas.1316909110>
- Ito, U., Kuroiwa, T., Nagasao, J., Kawakami, E., & Oyanagi, K. (2006). Temporal profiles of axon terminals, synapses and spines in the ischemic penumbra of the cerebral cortex: Ultrastructure of neuronal remodeling. *Stroke*, *37*(8), 2134–2139. <https://doi.org/10.1161/01.STR.0000231875.96714.b1>

- Jaillard, A., Martin, C. D., Garambois, K., Lebas, J. F., & Hommel, M. (2005). Vicarious function within the human primary motor cortex? *Brain*, *128*(5), 1122–1138.
<https://doi.org/10.1093/brain/awh456>
- Jara, J. H., Villa, S. R., Khan, N. A., Bohn, M. C., & Özdinler, P. H. (2012). AAV2 mediated retrograde transduction of corticospinal motor neurons reveals initial and selective apical dendrite degeneration in ALS. *Neurobiology of Disease*, *47*(2), 174–183.
<https://doi.org/10.1016/j.nbd.2012.03.036>
- Johnston, D. G., Denizet, M., Mostany, R., & Portera-Cailliau, C. (2013). Chronic in vivo imaging shows no evidence of dendritic plasticity or functional remapping in the contralesional cortex after stroke. *Cerebral Cortex (New York, N.Y.: 1991)*, *23*(4), 751–762. <https://doi.org/10.1093/cercor/bhs092>
- Jones, W. H., & Thomas, D. B. (1962). Changes in the dendritic organization of neurons in the cerebral cortex following deafferentation. *Journal of Anatomy*, *96*(Pt 3), 375–381.
- Joshi, I., & Andrew, R. D. (2001). Imaging anoxic depolarization during ischemia-like conditions in the mouse hemi-brain slice. *Journal of Neurophysiology*, *85*(1), 414–424.
<https://doi.org/10.1152/jn.2001.85.1.414>
- Joy, M. T., Ben Assayag, E., Shabashov-Stone, D., Liraz-Zaltsman, S., Mazzitelli, J., Arenas, M., Abduljawad, N., Kliper, E., Korczyn, A. D., Thareja, N. S., Kesner, E. L., Zhou, M., Huang, S., Silva, T. K., Katz, N., Bornstein, N. M., Silva, A. J., Shohami, E., & Carmichael, S. T. (2019). CCR5 Is a Therapeutic Target for Recovery after Stroke and Traumatic Brain Injury. *Cell*, *176*(5), 1143-1157.e13.
<https://doi.org/10.1016/j.cell.2019.01.044>

- Juttler, E., Kohrmann, M., & Schellinger, P. D. (2006). Therapy for early reperfusion after stroke. *Nature Clinical Practice Cardiovascular Medicine*, 3(12), 656–663.
<https://doi.org/10.1038/ncpcardio0721>
- Kanazawa, M., Ninomiya, I., Hatakeyama, M., Takahashi, T., & Shimohata, T. (2017). Microglia and Monocytes/Macrophages Polarization Reveal Novel Therapeutic Mechanism against Stroke. *International Journal of Molecular Sciences*, 18(10), 2135.
<https://doi.org/10.3390/ijms18102135>
- Karbowski, J., & Urban, P. (2023). Information encoded in volumes and areas of dendritic spines is nearly maximal across mammalian brains. *Scientific Reports*, 13(1), 22207.
<https://doi.org/10.1038/s41598-023-49321-9>
- Kirov, S. A., & Harris, K. M. (1999). Dendrites are more spiny on mature hippocampal neurons when synapses are inactivated. *Nature Neuroscience*, 2(10), 878–883.
<https://doi.org/10.1038/13178>
- Kleim, J. A., Hogg, T. M., VandenBerg, P. M., Cooper, N. R., Bruneau, R., & Remple, M. (2004). Cortical synaptogenesis and motor map reorganization occur during late, but not early, phase of motor skill learning. *The Journal of Neuroscience: The Official Journal of the Society for Neuroscience*, 24(3), 628–633.
<https://doi.org/10.1523/JNEUROSCI.3440-03.2004>
- Kokinovic, B., & Medini, P. (2018). Loss of GABA_B-mediated interhemispheric synaptic inhibition in stroke periphery. *The Journal of Physiology*, 596(10), 1949–1964.
<https://doi.org/10.1113/JP275690>

- Kuriakose, D., & Xiao, Z. (2020). Pathophysiology and Treatment of Stroke: Present Status and Future Perspectives. *International Journal of Molecular Sciences*, 21(20), 7609.
<https://doi.org/10.3390/ijms21207609>
- Lacoste, B., Comin, C. H., Ben-Zvi, A., Kaeser, P. S., Xu, X., Costa, L. da F., & Gu, C. (2014). Sensory-related neural activity regulates the structure of vascular networks in the cerebral cortex. *Neuron*, 83(5), 1117–1130. <https://doi.org/10.1016/j.neuron.2014.07.034>
- Latifi, S., Mitchell, S., Habibey, R., Hosseini, F., Donzis, E., Estrada-Sánchez, A. M., Nejad, H. R., Levine, M., Golshani, P., & Carmichael, S. T. (2020). Neuronal Network Topology Indicates Distinct Recovery Processes after Stroke. *Cerebral Cortex*, 30(12), 6363–6375.
<https://doi.org/10.1093/cercor/bhaa191>
- Lay, C. C., Davis, M. F., Chen-Bee, C. H., & Frostig, R. D. (2010). Mild sensory stimulation completely protects the adult rodent cortex from ischemic stroke. *PloS One*, 5(6), e11270.
<https://doi.org/10.1371/journal.pone.0011270>
- Lee, M.-C., Kim, R. G., Lee, T., Kim, J.-H., Lee, K.-H., Choi, Y.-D., Kim, H.-S., Cho, J., Park, J.-Y., & Kim, H.-I. (2020). Ultrastructural Dendritic Changes Underlying Diaschisis After Capsular Infarct. *Journal of Neuropathology & Experimental Neurology*, 79(5), 508–517. <https://doi.org/10.1093/jnen/nlaa001>
- Li, P., & Murphy, T. H. (2008). Two-photon imaging during prolonged middle cerebral artery occlusion in mice reveals recovery of dendritic structure after reperfusion. *The Journal of Neuroscience: The Official Journal of the Society for Neuroscience*, 28(46), 11970–11979. <https://doi.org/10.1523/JNEUROSCI.3724-08.2008>
- Li, S., Overman, J. J., Katsman, D., Kozlov, S. V., Donnelly, C. J., Twiss, J. L., Giger, R. J., Coppola, G., Geschwind, D. H., & Carmichael, S. T. (2010). An age-related sprouting

- transcriptome provides molecular control of axonal sprouting after stroke. *Nature Neuroscience*, 13(12), 1496–1504. <https://doi.org/10.1038/nn.2674>
- Li, Z., Li, Z., Xu, W., Li, Y., Wang, Q., Xu, H., Manyande, A., Wu, D., Feng, M., & Xiang, H. (2021). The connectome from the cerebral cortex to the viscera using viral transneuronal tracers. *American Journal of Translational Research*, 13(11), 12152–12167.
- Lichtman, J. W., & Colman, H. (2000). Synapse Elimination and Indelible Memory. *Neuron*, 25(2), 269–278. [https://doi.org/10.1016/S0896-6273\(00\)80893-4](https://doi.org/10.1016/S0896-6273(00)80893-4)
- Lim, D. H., Mohajerani, M. H., LeDue, J., Boyd, J., Chen, S., & Murphy, T. H. (2012). In vivo Large-Scale Cortical Mapping Using Channelrhodopsin-2 Stimulation in Transgenic Mice Reveals Asymmetric and Reciprocal Relationships between Cortical Areas. *Frontiers in Neural Circuits*, 6. <https://doi.org/10.3389/fncir.2012.00011>
- Lin, Y.-C., Phua, S. C., Lin, B., & Inoue, T. (2013). Visualizing molecular diffusion through passive permeability barriers in cells: Conventional and novel approaches. *Current Opinion in Chemical Biology*, 17(4), 663–671. <https://doi.org/10.1016/j.cbpa.2013.04.027>
- Liu, Z., Zhang, R. L., Li, Y., Cui, Y., & Chopp, M. (2009). Remodeling of the Corticospinal Innervation and Spontaneous Behavioral Recovery After Ischemic Stroke in Adult Mice. *Stroke*, 40(7), 2546–2551. <https://doi.org/10.1161/STROKEAHA.109.547265>
- Luo, L., Callaway, E. M., & Svoboda, K. (2008). Genetic dissection of neural circuits. *Neuron*, 57(5), 634–660. <https://doi.org/10.1016/j.neuron.2008.01.002>
- Majewska, A., & Sur, M. (2003). Motility of dendritic spines in visual cortex in vivo: Changes during the critical period and effects of visual deprivation. *Proceedings of the National Academy of Sciences*, 100(26), 16024–16029. <https://doi.org/10.1073/pnas.2636949100>

- Masurkar, A. V., Srinivas, K. V., Brann, D. H., Warren, R., Lowes, D. C., & Siegelbaum, S. A. (2017). Medial and Lateral Entorhinal Cortex Differentially Excite Deep versus Superficial CA1 Pyramidal Neurons. *Cell Reports*, *18*(1), 148–160.
<https://doi.org/10.1016/j.celrep.2016.12.012>
- Merino-Serrais, P., Plaza-Alonso, S., Hellal, F., Valero-Freitag, S., Kastanauskaite, A., Muñoz, A., Plesnila, N., & DeFelipe, J. (2023). Microanatomical study of pyramidal neurons in the contralesional somatosensory cortex after experimental ischemic stroke. *Cerebral Cortex*, *33*(4), 1074–1089. <https://doi.org/10.1093/cercor/bhac121>
- Mishra, A., Reynolds, J. P., Chen, Y., Gourine, A. V., Rusakov, D. A., & Attwell, D. (2016). Astrocytes mediate neurovascular signaling to capillary pericytes but not to arterioles. *Nature Neuroscience*, *19*(12), 1619–1627. <https://doi.org/10.1038/nn.4428>
- Mizrahi, A., Crowley, J. C., Shtoyerman, E., & Katz, L. C. (2004). High-resolution in vivo imaging of hippocampal dendrites and spines. *The Journal of Neuroscience: The Official Journal of the Society for Neuroscience*, *24*(13), 3147–3151.
<https://doi.org/10.1523/JNEUROSCI.5218-03.2004>
- Mostany, R., Chowdhury, T. G., Johnston, D. G., Portonovo, S. A., Carmichael, S. T., & Portera-Cailliau, C. (2010). Local Hemodynamics Dictate Long-Term Dendritic Plasticity in Peri-Infarct Cortex. *The Journal of Neuroscience*, *30*(42), 14116–14126.
<https://doi.org/10.1523/JNEUROSCI.3908-10.2010>
- Murphy, T. H., & Corbett, D. (2009). Plasticity during stroke recovery: From synapse to behaviour. *Nature Reviews. Neuroscience*, *10*(12), 861–872.
<https://doi.org/10.1038/nrn2735>

- Murphy, T. H., Li, P., Betts, K., & Liu, R. (2008). Two-photon imaging of stroke onset in vivo reveals that NMDA-receptor independent ischemic depolarization is the major cause of rapid reversible damage to dendrites and spines. *The Journal of Neuroscience: The Official Journal of the Society for Neuroscience*, 28(7), 1756–1772.
<https://doi.org/10.1523/JNEUROSCI.5128-07.2008>
- Nagendran, T., Larsen, R. S., Bigler, R. L., Frost, S. B., Philpot, B. D., Nudo, R. J., & Taylor, A. M. (2017). Distal axotomy enhances retrograde presynaptic excitability onto injured pyramidal neurons via trans-synaptic signaling. *Nature Communications*, 8(1), 625.
<https://doi.org/10.1038/s41467-017-00652-y>
- Nassi, J. J., Cepko, C. L., Born, R. T., & Beier, K. T. (2015). Neuroanatomy goes viral! *Frontiers in Neuroanatomy*, 9, 80. <https://doi.org/10.3389/fnana.2015.00080>
- Nimchinsky, E. A., Sabatini, B. L., & Svoboda, K. (2002). Structure and Function of Dendritic Spines. In *Annual Review of Physiology* (Vol. 64, Issue Volume 64, 2002, pp. 313–353). Annual Reviews. <https://doi.org/10.1146/annurev.physiol.64.081501.160008>
- Oh, S. W., Harris, J. A., Ng, L., Winslow, B., Cain, N., Mihalas, S., Wang, Q., Lau, C., Kuan, L., Henry, A. M., Mortrud, M. T., Ouellette, B., Nguyen, T. N., Sorensen, S. A., Slaughterbeck, C. R., Wakeman, W., Li, Y., Feng, D., Ho, A., ... Zeng, H. (2014). A mesoscale connectome of the mouse brain. *Nature*, 508(7495), 207–214.
<https://doi.org/10.1038/nature13186>
- Overman, J. J., Clarkson, A. N., Wanner, I. B., Overman, W. T., Eckstein, I., Maguire, J. L., Dinov, I. D., Toga, A. W., & Carmichael, S. T. (2012). A role for ephrin-A5 in axonal sprouting, recovery, and activity-dependent plasticity after stroke. *Proceedings of the National Academy of Sciences*, 109(33). <https://doi.org/10.1073/pnas.1204386109>

- Papadopoulos, C. M., Tsai, S.-Y., Cheatwood, J. L., Bollnow, M. R., Kolb, B. E., Schwab, M. E., & Kartje, G. L. (2006). Dendritic plasticity in the adult rat following middle cerebral artery occlusion and Nogo-a neutralization. *Cerebral Cortex (New York, N.Y.: 1991)*, *16*(4), 529–536. <https://doi.org/10.1093/cercor/bhi132>
- Prada, I., Gabrielli, M., Turola, E., Iorio, A., D'Arrigo, G., Parolisi, R., De Luca, M., Pacifici, M., Bastoni, M., Lombardi, M., Legname, G., Cojoc, D., Buffo, A., Furlan, R., Peruzzi, F., & Verderio, C. (2018). Glia-to-neuron transfer of miRNAs via extracellular vesicles: A new mechanism underlying inflammation-induced synaptic alterations. *Acta Neuropathologica*, *135*(4), 529–550. <https://doi.org/10.1007/s00401-017-1803-x>
- Rakic, P., Bourgeois, J.-P., & Goldman-Rakic, P. S. (1994). Synaptic development of the cerebral cortex: Implications for learning, memory, and mental illness. In J. Van Pelt, M. A. Corner, H. B. M. Uylings, & F. H. Lopes Da Silva (Eds.), *Progress in Brain Research* (Vol. 102, pp. 227–243). Elsevier. [https://doi.org/10.1016/S0079-6123\(08\)60543-9](https://doi.org/10.1016/S0079-6123(08)60543-9)
- Risher, W. C., Ard, D., Yuan, J., & Kirov, S. A. (2010). Recurrent spontaneous spreading depolarizations facilitate acute dendritic injury in the ischemic penumbra. *The Journal of Neuroscience: The Official Journal of the Society for Neuroscience*, *30*(29), 9859–9868. <https://doi.org/10.1523/JNEUROSCI.1917-10.2010>
- Saleeba, C., Dempsey, B., Le, S., Goodchild, A., & McMullan, S. (2019). A Student's Guide to Neural Circuit Tracing. *Frontiers in Neuroscience*, *13*, 897. <https://doi.org/10.3389/fnins.2019.00897>
- Saver, J. L. (2006). Time Is Brain—Quantified. *Stroke*, *37*(1), 263–266. <https://doi.org/10.1161/01.STR.0000196957.55928.ab>

- Schaffer, C. B., Friedman, B., Nishimura, N., Schroeder, L. F., Tsai, P. S., Ebner, F. F., Lyden, P. D., & Kleinfeld, D. (2006). Two-photon imaging of cortical surface microvessels reveals a robust redistribution in blood flow after vascular occlusion. *PLoS Biology*, *4*(2), e22. <https://doi.org/10.1371/journal.pbio.0040022>
- Shih, A. Y., Blinder, P., Tsai, P. S., Friedman, B., Stanley, G., Lyden, P. D., & Kleinfeld, D. (2013). The smallest stroke: Occlusion of one penetrating vessel leads to infarction and a cognitive deficit. *Nature Neuroscience*, *16*(1), 55–63. <https://doi.org/10.1038/nn.3278>
- Shih, A. Y., Friedman, B., Drew, P. K., Tsai, P. S., Lyden, P. D., & Kleinfeld, D. (2009). Active Dilation of Penetrating Arterioles Restores Red Blood Cell Flux to Penumbral Neocortex after Focal Stroke. *Journal of Cerebral Blood Flow & Metabolism*, *29*(4), 738–751. <https://doi.org/10.1038/jcbfm.2008.166>
- Silasi, G., & Murphy, T. H. (2014). Stroke and the Connectome: How Connectivity Guides Therapeutic Intervention. *Neuron*, *83*(6), 1354–1368. <https://doi.org/10.1016/j.neuron.2014.08.052>
- Sporns, O., Tononi, G., & Kötter, R. (2005). The Human Connectome: A Structural Description of the Human Brain. *PLoS Computational Biology*, *1*(4), e42. <https://doi.org/10.1371/journal.pcbi.0010042>
- Starkey, M. L., Bleul, C., Zörner, B., Lindau, N. T., Mueggler, T., Rudin, M., & Schwab, M. E. (2012). Back seat driving: Hindlimb corticospinal neurons assume forelimb control following ischaemic stroke. *Brain*, *135*(11), 3265–3281. <https://doi.org/10.1093/brain/aws270>

- Stroemer, R. P., Kent, T. A., & Hulsebosch, C. E. (1995). Neocortical Neural Sprouting, Synptogenesis, and Behavioral Recovery After Neocortical Infarction in Rats. *Stroke*, 26(11), 2135–2144. <https://doi.org/10.1161/01.STR.26.11.2135>
- Strong, A. J., Anderson, P. J., Watts, H. R., Virley, D. J., Lloyd, A., Irving, E. A., Nagafuji, T., Ninomiya, M., Nakamura, H., Dunn, A. K., & Graf, R. (2006). Peri-infarct depolarizations lead to loss of perfusion in ischaemic gyrencephalic cerebral cortex. *Brain*, 130(4), 995–1008. <https://doi.org/10.1093/brain/awl392>
- Takano, T., Tian, G.-F., Peng, W., Lou, N., Lovatt, D., Hansen, A. J., Kasischke, K. A., & Nedergaard, M. (2007). Cortical spreading depression causes and coincides with tissue hypoxia. *Nature Neuroscience*, 10(6), 754–762. <https://doi.org/10.1038/nn1902>
- Takatsuru, Y., Nakamura, K., & Nabekura, J. (2013). Compensatory contribution of the contralateral pyramidal tract after experimental cerebral ischemia. *Frontiers of Neurology and Neuroscience*, 32, 36–44. <https://doi.org/10.1159/000346409>
- Tervo, D. G. R., Hwang, B.-Y., Viswanathan, S., Gaj, T., Lavzin, M., Ritola, K. D., Lindo, S., Michael, S., Kuleshova, E., Ojala, D., Huang, C.-C., Gerfen, C. R., Schiller, J., Dudman, J. T., Hantman, A. W., Looger, L. L., Schaffer, D. V., & Karpova, A. Y. (2016). A Designer AAV Variant Permits Efficient Retrograde Access to Projection Neurons. *Neuron*, 92(2), 372–382. <https://doi.org/10.1016/j.neuron.2016.09.021>
- Tjia, M., Yu, X., Jammu, L. S., Lu, J., & Zuo, Y. (2017). Pyramidal Neurons in Different Cortical Layers Exhibit Distinct Dynamics and Plasticity of Apical Dendritic Spines. *Frontiers in Neural Circuits*, 11. <https://www.frontiersin.org/journals/neural-circuits/articles/10.3389/fncir.2017.00043>

- Trachtenberg, J. T., Chen, B. E., Knott, G. W., Feng, G., Sanes, J. R., Welker, E., & Svoboda, K. (2002). Long-term in vivo imaging of experience-dependent synaptic plasticity in adult cortex. *Nature*, *420*(6917), 788–794. <https://doi.org/10.1038/nature01273>
- Tu, X., Li, X., Zhu, H., Kuang, X., Si, X., Zou, S., Hao, S., Huang, Y., & Xiao, J. (2022). Unilateral cerebral ischemia induces morphological changes in the layer V projection neurons of the contralateral hemisphere. *Neuroscience Research*, *182*, 41–51. <https://doi.org/10.1016/j.neures.2022.06.007>
- Tyan, Y.-S., Liao, J.-R., Shen, C.-Y., Lin, Y.-C., & Weng, J.-C. (2017). Gender differences in the structural connectome of the teenage brain revealed by generalized q-sampling MRI. *NeuroImage: Clinical*, *15*, 376–382. <https://doi.org/10.1016/j.nicl.2017.05.014>
- Urbin, M. A., Hong, X., Lang, C. E., & Carter, A. R. (2014). Resting-State Functional Connectivity and Its Association With Multiple Domains of Upper-Extremity Function in Chronic Stroke. *Neurorehabilitation and Neural Repair*, *28*(8), 761–769. <https://doi.org/10.1177/1545968314522349>
- Wahl, A. S., Büchler, U., Brändli, A., Brattoli, B., Musall, S., Kasper, H., Ineichen, B. V., Helmchen, F., Ommer, B., & Schwab, M. E. (2017). Optogenetically stimulating intact rat corticospinal tract post-stroke restores motor control through regionalized functional circuit formation. *Nature Communications*, *8*(1), 1187. <https://doi.org/10.1038/s41467-017-01090-6>
- Wang, H., He, Y., Sun, Z., Ren, S., Liu, M., Wang, G., & Yang, J. (2022). Microglia in depression: An overview of microglia in the pathogenesis and treatment of depression. *Journal of Neuroinflammation*, *19*(1), 132. <https://doi.org/10.1186/s12974-022-02492-0>

- Watson, B. D., Dietrich, W. D., Busto, R., Wachtel, M. S., & Ginsberg, M. D. (1985). Induction of reproducible brain infarction by photochemically initiated thrombosis. *Annals of Neurology*, *17*(5), 497–504. <https://doi.org/10.1002/ana.410170513>
- Werhahn, K. J., Conforto, A. B., Kadom, N., Hallett, M., & Cohen, L. G. (2003). Contribution of the ipsilateral motor cortex to recovery after chronic stroke. *Annals of Neurology*, *54*(4), 464–472. <https://doi.org/10.1002/ana.10686>
- Winship, I. R., & Murphy, T. H. (2008). In Vivo Calcium Imaging Reveals Functional Rewiring of Single Somatosensory Neurons after Stroke. *Journal of Neuroscience*, *28*(26), 6592–6606. <https://doi.org/10.1523/JNEUROSCI.0622-08.2008>
- Yu, C.-L., Zhou, H., Chai, A.-P., Yang, Y.-X., Mao, R.-R., & Xu, L. (2015). Whole-scale neurobehavioral assessments of photothrombotic ischemia in freely moving mice. *Journal of Neuroscience Methods*, *239*, 100–107. <https://doi.org/10.1016/j.jneumeth.2014.10.004>
- Yu, X., & Zuo, Y. (2011). Spine plasticity in the motor cortex. *Current Opinion in Neurobiology*, *21*(1), 169–174. <https://doi.org/10.1016/j.conb.2010.07.010>
- Yuste, R. (2011). Dendritic spines and distributed circuits. *Neuron*, *71*(5), 772–781. <https://doi.org/10.1016/j.neuron.2011.07.024>
- Yuste, R., & Bonhoeffer, T. (2004). Genesis of dendritic spines: Insights from ultrastructural and imaging studies. *Nature Reviews Neuroscience*, *5*(1), 24–34. <https://doi.org/10.1038/nrn1300>
- Zhang, S., Boyd, J., Delaney, K., & Murphy, T. H. (2005). Rapid reversible changes in dendritic spine structure in vivo gated by the degree of ischemia. *The Journal of Neuroscience*:

The Official Journal of the Society for Neuroscience, 25(22), 5333–5338.

<https://doi.org/10.1523/JNEUROSCI.1085-05.2005>

Zhang, S., & Murphy, T. H. (2007). Imaging the Impact of Cortical Microcirculation on Synaptic Structure and Sensory-Evoked Hemodynamic Responses In Vivo. *PLOS Biology*, 5(5), e119. <https://doi.org/10.1371/journal.pbio.0050119>

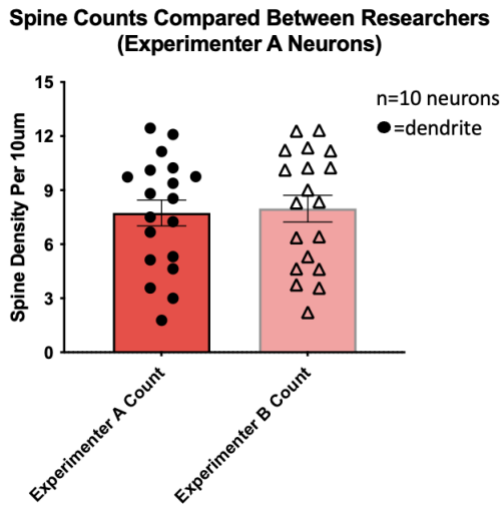
Zhang, Y., Lian, L., Fu, R., Liu, J., Shan, X., Jin, Y., & Xu, S. (2022). Microglia: The Hub of Intercellular Communication in Ischemic Stroke. *Frontiers in Cellular Neuroscience*, 16. <https://www.frontiersin.org/journals/cellular-neuroscience/articles/10.3389/fncel.2022.889442>

Zingg, B., Hintiryan, H., Gou, L., Song, M. Y., Bay, M., Bienkowski, M. S., Foster, N. N., Yamashita, S., Bowman, I., Toga, A. W., & Dong, H.-W. (2014). Neural Networks of the Mouse Neocortex. *Cell*, 156(5), 1096–1111. <https://doi.org/10.1016/j.cell.2014.02.023>

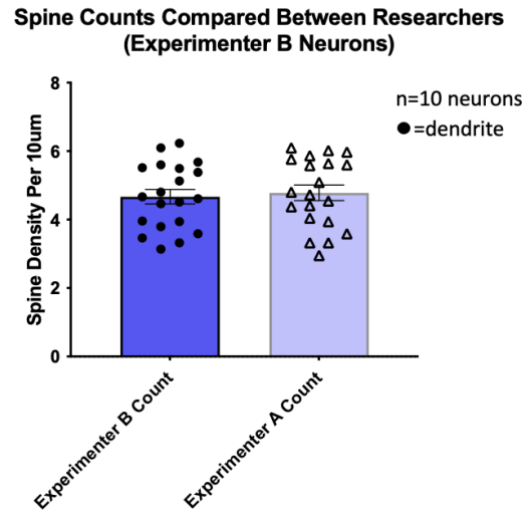
Zuo, Y., Lin, A., Chang, P., & Gan, W.-B. (2005). Development of Long-Term Dendritic Spine Stability in Diverse Regions of Cerebral Cortex. *Neuron*, 46(2), 181–189. <https://doi.org/10.1016/j.neuron.2005.04.001>

Appendix

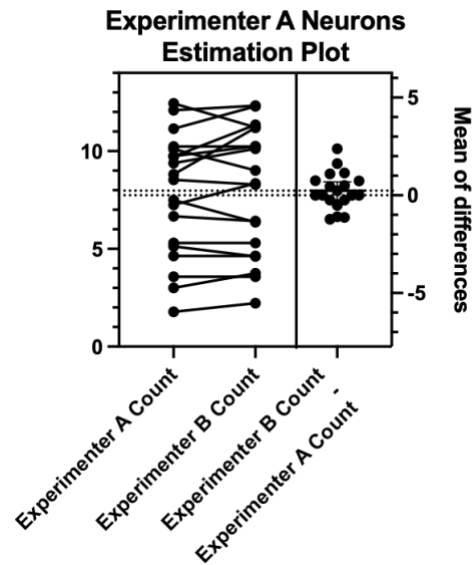
A.



B.



C.



D.

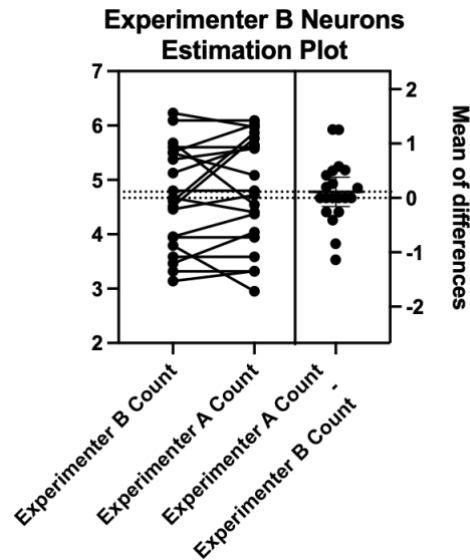


Figure 13: No significant difference in dendritic spine density counts between researchers
A. Dendritic spine counts did not differ between Experimenter A and Experimenter B for Experimenter A's neurons. **B.** Dendritic spine counts did not differ between Experimenter B and Experimenter A for Experimenter B's neurons. **C.** Estimation plot comparing Experimenter A counts and Experimenter B counts for dendritic spine density of Experimenter A's neurons. **D.** Estimation plot comparing Experimenter B counts and Experimenter A counts for dendritic spine density of Experimenter B's neurons. Error bars: mean±SEM.

Table 4: Summary of neurons counted in superficial and deep cortical layers per brain 1-week post-sham and stroke

One Week Sham					One Week Stroke				
Mouse ID	Area	# Neurons Imaged	Superficial	Deep	Mouse ID	Area	# Neurons Imaged	Superficial	Deep
M-ADAM17-E2	M1	5	3	2	F-C57-GK-N3 Stroke	M1	5	1	4
	S1FL	5	2	3		Peri	5	3	2
	S2	5	2	3		S2	5	2	3
	Contra S1FL	0	0	0		Contra Peri	5	2	3
F-C57-G0-N1 Sham	M1	6	4	2	M-C57-GR-N0 Stroke	M1	5	2	3
	S1FL	5	3	2		Peri	5	3	2
	S2	5	2	3		S2	5	2	3
	Contra S1FL	5	4	1		Contra Peri	5	0	5
M-C57-GP-N0 Sham	M1	5	2	3	M-C57-GP-N1 Stroke	M1	5	4	1
	S1FL	5	2	3		Peri	5	3	2
	S2	5	3	2		S2	5	1	4
	Contra S1FL	5	2	3		Contra Peri	5	2	3
M-C57-GR-N1 Sham	M1	5	3	2	F-C57-GN-N1 Stroke	M1	5	2	3
	S1FL	5	2	3		Peri	5	5	0
	S2	5	2	3		S2	5	4	1
	Contra S1FL	5	5	0		Contra Peri	5	5	0
F-C57-G0-N0 Sham	M1	5	1	4	F-C57-GK-N0 Stroke	M1	5	1	4
	S1FL	5	1	4		Peri	5	2	3
	S2	5	0	5		S2	5	2	3
	Contra S1FL	5	2	3		Contra Peri	5	4	1
F-C57-HA-N0 Sham	M1	5	3	2	M-C57-HC-N3 Stroke	M1	5	2	3
	S1FL	5	2	3		Peri	5	2	3
	S2	5	2	3		S2	5	2	3
	Contra S1FL	5	3	2		Contra Peri	5	3	2
M-C57-GP-N4 Sham	Contra S1FL	5	2	3					

Table 5: Summary of neurons counted in superficial and deep cortical neurons per brain 6-weeks post-sham and stroke

Six Week Sham					Six Week Stroke				
Mouse ID	Area	# Neurons Imaged	Superficial	Deep	Mouse ID	Area	# Neurons Imaged	Superficial	Deep
F-C57-GQ-N0 Sham	M1	5	2	3	F-C57-GQ-N1 Stroke	M1	5	2	3
	S1FL	5	2	3		Peri	5	2	3
	S2	5	2	3		S2	5	2	3
	Contra S1FL	5	3	2		Contra Peri	5	2	3
F-C57-GQ-N3 Sham	M1	5	0	5	F-C57-HA-N1 Stroke	M1	5	3	2
	S1FL	5	3	2		Peri	5	2	3
	S2	5	3	2		S2	5	2	3
	Contra S1FL	3	2	1		Contra Peri	5	3	2
M-C57-HC-N1 Sham	M1	5	2	3	F-C57-HA-N3 Stroke	M1	5	0	5
	S1FL	5	2	3		Peri	5	0	5
	S2	5	2	3		S2	5	0	5
	Contra S1FL	5	2	3		Contra Peri	5	4	1
M-C57-HW-N0 Stroke	M1	5	3	2	M-C57-HW-N6 Stroke	M1	5	2	3
	Peri	5	3	2		Peri	5	2	3
	S2	5	3	2		S2	5	2	3
	Contra Peri	5	3	2		Contra Peri	5	3	2